THESIS APPROVAL

GRADUATE SCHOOL, KASETSART UNIVERSITY

Master of Engineering (Chemical Engineering)

DEGREE

Chemical Engineering	Chemical Engineering
FIELD	**DEPARTMENT**

TITLE: Simulation Spray Drying of Milk Powder using Computational Fluid Dynamics

NAME: Miss Pornpen Nualnuk

THIS THESIS HAS BEEN ACCEPTED BY

THESIS ADVISOR

(Associate Professor Thongchai Srinophakun, Ph.D.)

THESIS CO-ADVISOR

(Miss Chalida Niamnuy, D.Eng.)

DEPARTMENT HEAD

(Associate Professor Apinya Duangchan, Ph.D.)

APPROVED BY THE GRADUATE SCHOOL ON _____

DEAN

(Associate Professor Gunjana Theeragool, D.Agr.)

THESIS

SIMULATION SPRAY DRYING OF MILK POWDER USING COMPUTATIONAL FLUID DYNAMICS

PORNPEN NUALNUK

A Thesis Submitted in Partial Fulfillment of
the Requirements for the Degree of
Master of Engineering (Chemical Engineering)
Graduate School, Kasetsart University
2011

Pornpen Nualnuk 2011: Simulation Spray Drying of Milk Powder using Computational Fluid Dynamics. Master of Engineering (Chemical Engineering), Major Field: Chemical Engineering, Department of Chemical Engineering. Thesis Advisor: Associate Professor Thongchai Srinophakun, Ph.D. 89 pages.

The drying of skim milk in a spray dryer was simulated using computational fluid dynamics (CFD) method. The theoretical model of the process was based on two-phase Eulerian-Lagrangian approach for gas and droplet in the spray drying process The objective of the current study was to simulate air flow, temperature profile, and residence time distibution for skim milk powder in spray dryer. In addition, the stickiness of skim milk powder was also investigated. The spray drying model was divided into five major parts. The first part was the model to validate with the experiment data of Kieveit (1997) for the accuracy of the model. The second part was the model to predict the air flow pattern. The third part was the model to predict the particle residence time distribution. The forth part was the model to predict the occurrence of stickiness in the spray drying. The last part was created in spray drying process. Good agreement was obtained with the published experiment data where the CFD simulation correctly predicted a fast downward central flowing core and slow recirculation zones near the wall. The increment of the mean droplet size caused a decrease in the particle residence time distribution because of the results from gravity force. The increment of the mean droplet size caused an increase in the stickiness rate. The spray model simulation can be used the predict to particle motion inside spray chamber and also to explain the stickiness in skim milk powder during spray drying process.

_____ _____ ____ /____ /____

Student's signature Thesis Advisor's signature

ACKNOWLEDGEMENTS

It is my pleasure to acknowledge those who have helped make this thesis possible. I would like to express my gratitude to my advisor, Associate Professor Thongchai Srinophakun for advice, valuable suggestion, encouragement, enthusiasm, and great support throughout this work. He has been my most important mentor, and has greatly influenced my perspective in process control.

Appreciation is also extended to Dr. Chalida Niamnuy, Assistant Professor Sittinun Thorkaew, and Associate Professor Sirikalaya Suvachitanont for my kindly committee and giving me useful recommendations.

Acknowledgement is given to the Graduate school, Kasetsart University for giving me the scholarship to implement the research, given to the Department of Chemical Engineering, Kasetsart University for all facilities provided to accomplish this thesis, and also given to the Centre of Excellence for Petroleum, Petrochemicals, and Advanced Materials; Centre for Advanced Studies in Industrial Technology, for supporting this research.

My sincere thank is also given to my friends, colleagues, and teams in Center of Process Control and Operation (CPCO), Kasetsart University, Thailand.

Pornpen Nualnuk

April 2011

TABLE OF CONTENTS

Pages

LIST OF TABLES

LIST OF FIGURES

LIST OF FIGURES (Continued)

LIST OF ABBREVIATIONS

Abbreviations

SMP	=	skim milk powder
WMP	=	whole milk powder
MPC	=	milk protein concentrate
CFD	=	Computational Fluid Dynamics
DPM	=	Discrete Phase Model
RSM	=	Reynolds Stress Model

Greek Letters

σ	=	surface tension
ρ	=	gas density
μ	=	viscosity
ε	=	turbulence energy dissipation rate
k	=	turbulence kinetic energy
μ_t	=	turbulent viscosity

Subscripts

g	=	gas
p	=	particle/droplet
s	=	surface
C	=	constant

Variables

A_p	=	surface area of the droplet
C_D	=	drag coefficient

LIST OF ABBREVIATIONS (Continued)

Y_s	=	saturation humidity
Y_g	=	gas humidity
k_c	=	mass transfer coefficient
$\underline{v}$	=	gas phase velocity
$\underline{u}_p$	=	particle phase velocity
ρ_g	=	density of the gas
ρ_p	=	density of the particle
Re	=	Reynolds number
d_p	=	particle diameter
m_p	=	mass of the particle
c_p	=	particle heat capacity
T_p	=	particle temperature
h_{fg}	=	latent heat
h	=	heat transfer coefficient
Pr	=	Prandtl number
k_{ta}	=	thermal conductivity of the gas
m	=	molecular viscosity of the gas
Sh	=	Sherwood number
$D_{i,m}$	=	diffusion coefficient
Sc	=	Schmidt number
C_p	=	Specific heat capacity
t	=	Time

SIMULATION SPRAY DRYING OF MILK POWDER USING COMPUTATIONAL FLUID DYNAMICS

INTRODUCTION

Spray drying is a process to convert small liquid droplets into dried powder in contact with hot air. Rapid evaporation maintains droplet temperature at low level, so that high drying air temperatures can be applied without affecting the product quality. Stickiness is the phenomenon that commonly encounter during spray drying of milk powder. This is very important in the spray drying process. Better understanding of this phenomenon can be achieved by spray drying model of agglomeration process. In this thesis, heat and mass transfer of droplet, and Discrete Phase Model (DPM) simultaneously with Computational Fluid Dynamics (CFD) were used to describe the air flow pattern, particle residence time and stickiness process of skim milk powder during spray drying process.

Milk powder is a manufactured dairy product made by evaporating water in milk. It consists mainly of fat, protein, and lactose. The purpose of drying milk is to preserve shelf life of milk for later consumption, due to its low moisture content. Moreover, it is easy for transportation due to the reducing of milk bulk. The common milk powders are skim milk powder (SMP), whole milk powder (WMP), and milk protein concentrate (MPC). Milk powders of various types are used in a wide range of products such as baked goods, snacks and soups, chocolates and confectionary, ice cream, nutritional products, recombined milks and other liquid beverages.

The major technology used for milk powder production is a spray drying. Spray drying can produce dry powder from liquid or slurry by rapidly drying the milk droplet with a hot gas. This is the preferred technique for drying of many thermally-sensitive materials such as foods and pharmaceuticals. Moreover, this technique may be used as an alternative method for crystallization of amorphous powders during the drying process as a result of the temperature effects on the amorphous powders. In

milk powder processing, milk is instantly dehydrated, producing fine particles of powdered milk solids without any loss of nutritive value.

Computational Fluid Dynamics (CFD) is a technique that is used to determine the numerical solution for describing the system of fluid flow, heat and mass transfer, and associated phenomena by mean of computer-based simulation (Versteeg, 1995).The physical aspects of any fluid flow are governed by three fundamental principles: Mass is conserved, Newton's second law is conserved and Energy is conserved. These fundamental principles can be expressed in terms of mathematical equations. The set of equations that describe the processes of momentum, heat and mass transfer are known as the Navier-Stokes equations, which are partial differential equations. They are cannot be solved to obtain the general analytical solution but they can be discretised and solved numerically. In CFD technique, the flow region is divided into a large number of finite volumes or cells. The governing partial differential equations are discretised using a wide range of techniques such as finite difference, finite volume or finite element. Each technique has its own mathematical basis but deal with the same fundamental physical relationships of fluid flow. The most common is known as the finite volume method.

.

OBJECTIVES

The objective of the thesis study was to simulate air flow, temperature profile and residence time distibution for skim milk powder in spray dryer. In addition, the stickiness of skim milk powder also was investigated.

Scope of Work

The scopes of this work are as follow:

1.Using Computational Fluid Dynamics for prediction of air flow pattern and temperature profile in skim milk powder during spray drying process.

2. Formulate spray drying model for prediction particle residence time distibution on the process of spray drying.

3. The spray drying model to prediction of stickiness.

4. The plant was created in spray drying process.

Thesis Contribution

The expected result of this thesis is the understanding of stickiness in milk powder. In addition, the developed spray model can be used to predict to particle motion inside spray chamber and also explain the stickiness process in skim milk powder during spray drying process.

LITERATURE REVIEW

1. Milk powder

Milk powder is made by evaporating milk to dryness. It contains all twenty standard amino acids and is high in soluble vitamins and minerals. However, the major components of milk powder are fat, protein, and lactose. Milk powder is frequently used in the manufacture of infant formula, confectionery such as chocolate and caramel candy, and in recipes for baked goods. (Pietsch, 2003).

1.1 Types of milk powder

There are many types of milk powder produced today. They are different in the composition of fat, protein, and lactose containing in milk and their shelf life. The common types of milk powder are skim milk powder (SMP), whole milk powder (WMP), and milk protein concentrate (MPC). Skim milk powder (SMP) has nearly all the fat removed which has a fat content of between 0.1-0.3 percent. It contains slightly more calcium than whole milk and lower levels of fat soluble vitamins, particularly vitamin A, as this is lost when the fat is removed. Moreover, it can be kept for up to one year if stored correctly. For whole milk powder (WMP), it contains all the nutrients of whole milk in a concentrated form with the exception of vitamin C, thiamin and vitamin B12. Milk protein concentrate (MPC) is highly nutritional product manufactured from fresh skim milk with low lactose level. The level of protein, lactose and minerals presented depends on the degree of protein concentration.

Most of the milk powder in the market is made from skim milk. The whole milk powder can also produce, but the powder itself does not keep well on account of its high content of butterfat, averaging about 30 percent. This will make whole milk powder to become rancid, especially if copper or iron were picked up during the manufacturing process.

1.2 Milk powder manufacturing

Milk powder manufacture is a simple process which involves the step of removal of water under strict hygiene conditions while retaining all the desirable natural properties of the milk such as color, flavor, solubility, and nutritional value. Milk powders may vary in their gross composition such as milk fat, protein, and lactose, the heat treatment they receive during manufacture, powder particle size and packaging. The milk powder manufacturing diagram is shown in the Figure 1.

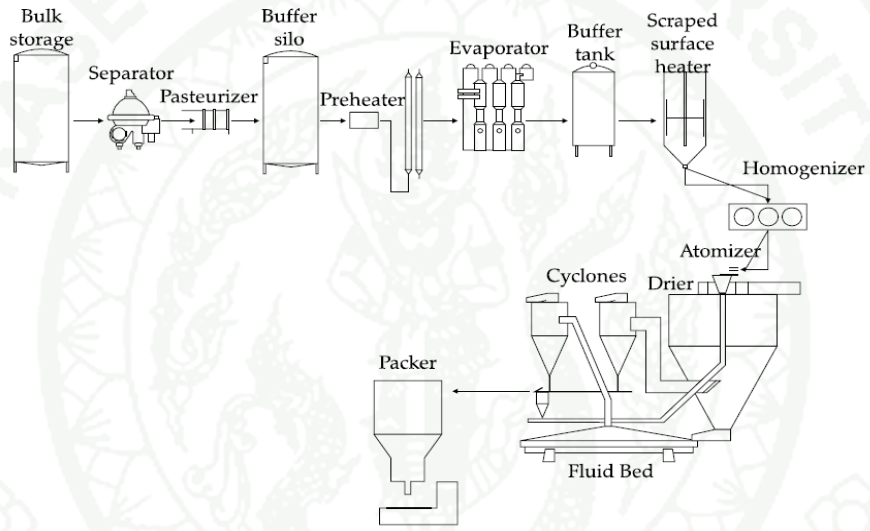

Figure 1 Milk powder manufacturing diagram

Source: Chem Processes dairy (2009)

The production of milk powder starts with pasteurizing raw milk from dairy factory and separating it into skim milk and cream using a centrifugal cream separator. The standardized milk is heated to temperatures between 75 and 120 ^{o}C in the preheater. Milk is concentrated by the evaporator before sending to the spray dryer. Spray drying involves atomizing the milk concentrate from the evaporator into fine droplets. The powder particles leave the spray dryer at the bottom into the fluid bed. Most of the air leaves the spray chamber to a cyclone where the small powder particles are separated from the outlet air. Powder particles separated by a cyclone can be reintroduced into the spray chamber or into the fluid bed for the particle size

enlargement process. The powder particles collected from the fluid bed and cyclone are passed through the screw conveyor and sent to the packer.

2. Spray drying

Spray drying is a process to convert small liquid droplets into dried powder in contact with hot air. Rapid evaporation maintains droplet temperature at low level, so that high drying air temperatures can be applied without affecting the product quality. The drying time of the droplets in spray dryer is very short in comparison with most other drying processes. There are many type of dryer such as constant bed dryer, fluidize bed dryer and microwave dryer that used hot air flow for drying foods. Hot air contacts with solid products such as grains, vegetables and fruits pulps and dry them. These dryers need long time for drying processes. Low product temperature and short drying time allow spray drying of very heat sensitive products such as foods, dairy products and fruit juices.

2.1 Spray drying process

Spray drying is the process of atomization a solution or suspension into fine droplets followed by evaporation of water or other solvents containing in these droplets. It is used for the manufacture of many consumer and industrial products such as instant food products such as milk powder, instant beverage such as coffee, pharmaceuticals, ceramics, laundry detergents and agrochemicals. Spray drying is a widely used industrial process for the continuous production of dry powders with low moisture content As shown in Figure 2 the process stages of spray drying of operation (1) atomisation of liquid feed into a spray chamber (2) contact between the spray and the drying medium (3) moisture evaporation and (4) separation of dried products from air stream.

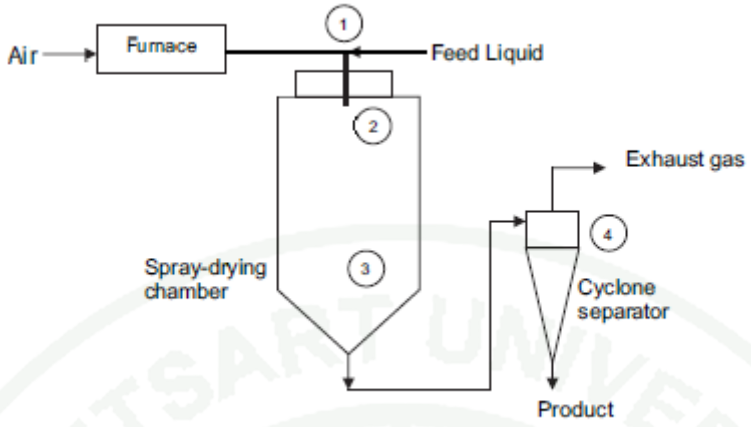

Figure 2 The process stages of spray drying

Source: Spray Drying (2009)

In the spray chamber, the incoming slurry or liquid solution is sprayed by rotary wheel atomizers or pressure nozzles atomization in a fine mist and dried by the hot air introduced at the top or bottom of producing fine droplets. These different styles of atomizers have different advantages and disadvantages depending on the application of the spray drying required, for example, a spray nozzle is used in place of an atomizer for a different dispersion rate. A nozzle is usually used to make the droplets as small as possible which maximize heat transfer and the rate of water vaporizes. Droplet sizes can range from 40 μm to 100 μm depending on the nozzle.

The flow of liquid and gas may be co-current, countercurrent, or a combination of both in the same unit. In the co-current flow, the particles will have a lower residence time within the system and the cyclone which is the particle separator device will operate more efficiently. However, in the counter-current flow method, the particles will have a greater residence time in the chamber and the spray dryer is usually used with a fluidized bed system. In the drying chamber, moisture is rapidly vaporized from the particle droplet producing residual particles of dry solid. The gas from the spray drying chamber passes through a cyclone separator where any entrained particles of solid (milk powder) are removed. Much of the dry solid settles

out of the gas into the bottom of drying chamber, from which it is removed by a rotary valve and screw conveyor and combined with any solid collected in the cyclone.

The advantage of spray drying is the product is dry very quickly compared to other methods of drying. Moreover, it also turns a solution or slurry into a dried powder in a single step, which can maximize profit and make the process simplification such as it can combine the functions of an evaporator, a crystallizer, a dryer, a size reduction unit, and a classifier in one unit (McCabe, 1993).

2.2 Drying kinetics for a single droplet

Spray drying refers to the process of thermally removing volatile liquid and finally produces a solid product. As soon as droplets of the spray come into contact with the drying air, evaporation takes place from the saturated vapor film which is quickly established at the droplet surface. Therefore, heat and mass transfer should be considered for operation. Normally, the drying kinetics of a single droplet which contains solid can be divided into two stages due to its morphology. In the first drying stage in Figure 3 the droplet with initial diameter has greatest amount of liquid when it enters the drying medium. Then, the evaporation of moisture at the droplet surface occur which results in shrinkage of droplet diameter. When the amount of liquid decreases to the critical value, a very thin layer of a dry solid crust forms at the outer surface of the droplet which is point 2 in this figure 3. At this point, the second drying stage begins and the droplet is treated onwards as a wet particle with a constant outer diameter. From this step, the wet particle includes two separated regions which are solid crust having a porous structure and wet core consisting of liquid and solid. During the second drying stage, due to the simultaneous heat transfer to the wet particle and mass transfer to the drying agent the thickness of the solid crust continuously increases. However, the diameter of wet core shrinks. Finally, the drying stops when the amount of the liquid decreases until reach the desired value.

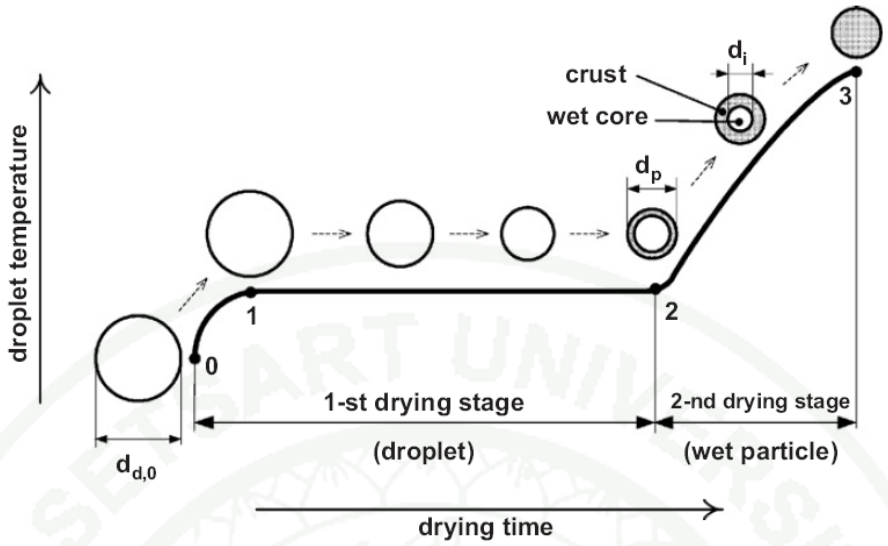

Figure 3 Typical temperature curve and morphological changes during drying of single droplet containing solid

Source: Spray Drying (2009)

Ferrari *et al*., 1989 studied the drying kinetics for a single droplet of skim milk. They developed the mathematical model to describe the drying behavior of a single droplet. The water concentration profiles inside the droplet and the droplet temperature were investigated during drying process by coupling mass and heat transfer equations. The transport of water in the liquid phase was described in terms of diffusion, which can be regarded as the controlling mechanism in many drying processes. The concentration profiles are dependent on the internal water diffusivity coefficient, D_w which is greatly affected by water concentration and temperature inside the droplet.

Chen *et al*., 2004 did the experiment to study the small droplet drying behavior. Whole milk powder was selected to study in this work. The isothermal drying of milk droplets has been obtained from the experiment. Moreover, the result from the experiment was used to validate with the results predicted from the conventional characteristic drying rate curve model (CDRC) and the reaction engineering approach model.

Mezhericher *et al*., 2008 proposed the theoretical model which consider the fully unsteady character of both heat and mass transfer during the drying of single droplet/wet particle. Moreover, this model enabled the prediction of pressure and fraction distribution of air-vapor mixture within the capillary pores of the wet particle crust. The silica droplet was studied in this work. The results showed a permanent rising of pressure within the capillary pores and this model can predict the pressure build-up and temperature rising within the particle wet core.

2.3 Types of atomizer

Atomization is the process of discharging the liquid at high velocity into a relatively slow moving stream air or gas or exposing a relatively slow moving liquid to a high velocity air stream. There are many types of atomizer which are different in their functions and the droplet size produced. However, there are two main types which are pressure atomizer and rotary atomizer. In pressure atomizer, the pressure energy is converted into kinetic energy to achieve a high relative velocity when a liquid is discharge through a small aperture under high applied pressure. Most of the atomizers in general use are of this type. They include plain orifice, pressure nozzle, dual orifice, and fan spray. For rotary atomizer, it consists of a high speed rotating surface with means for introducing liquid at its center. The rotating surface spreads out fairly uniformly under the action of centrifugal force. . It can be in the form of a flat disk, vaned disk, cup, or slotted wheel to guide the liquid to the periphery. The liquid flows radially outward across the rotating surface and is discharged at high velocity from its periphery (Lefebvre, 1989).

2.4 Stickiness

Stickiness is a phenomenon that reflects the tendency of some materials to agglomerate or adhere to contact surfaces. A low moisture or free flowing powder is first transformed into lumps, then into an agglomerated solid and ultimately into a sticky material. These phenomena result in loss of functionality and lowered quality of powder. They occur when sufficient viscous flow begins to form a liquid bridge

between two particle surfaces at their contact point or between the particle surface and another surface such as a spray dryer wall. The viscous flow of particle is governed by the temperature and water content in the particle and it is driven by surface energy.

In milk powder, the development of stickiness is a time, temperature and humidity that are related to the amorphous state of lactose and its glass transition temperature (T_g). With time, stickiness can cause caking due to the solidification of the liquid bridges by the crystallization of the amorphous lactose. Amorphous lactose is sticking when its T_g is exceeded sufficiently to make viscosity decrease, allowing viscous flow of the amorphous material and liquid bridge to develop between particles. The degree of stickiness of the powder has been correlated with the particle size and the amount of amorphous lactose present in the milk powder. The rate of stickiness development in amorphous lactose powder is a function of how much the temperature of the powder exceeds the amorphous lactose glass transition temperature, $T–T_g$.

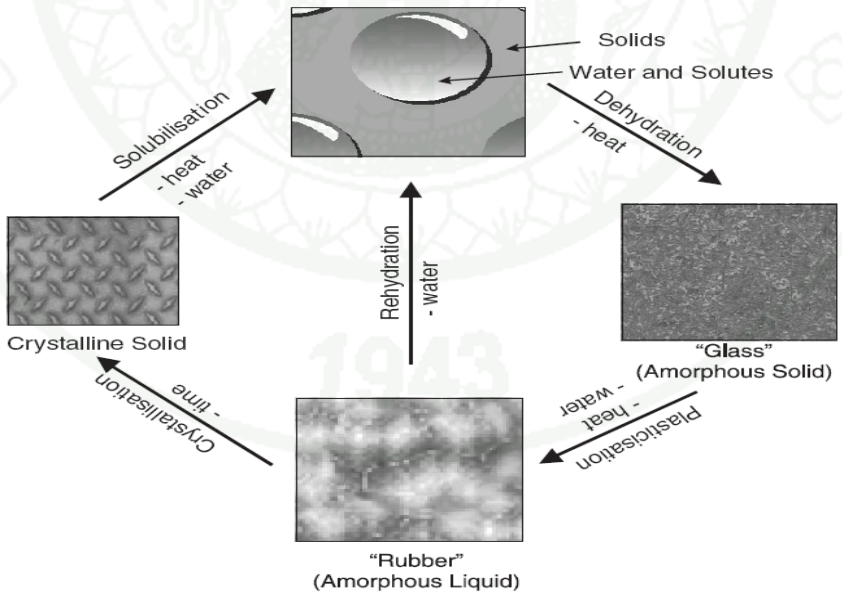

Figure 4 Formation of amorphous structures in dehydration process

Source: Roos (2002)

At the temperature below the T_g , an amorphous material behaves as a glass with a very high viscosity due to the limited of molecular movement at low temperature. However, the molecules are able to rearrange their structures from the unorganized structure of the amorphous solid in the glassy state to a viscous liquid state at the temperature above the T_g which allow viscous flow and sticking to occur under this condition. Eventually, the molecules will rearrange themselves to form a crystalline structure and solid bridges which cause a hard cake material.

Stickiness has a negative impact on the drying process except in the agglomeration operation, where cohesion is essential to bind particles. In spray drying, for example, stickiness can lead to reduced sensory characteristics due to thermal degradation as well as to lower product yields, operating problems, and fire and explosion hazards. Since this phenomenon has been recognized as significant problems that commonly encounter during spray drying process, many researchers have been interested in this phenomenon. They used the concept of the glass transition temperature to explain the initiation of stickiness in powder. However, most of them studied the stickiness phenomenon through the experiment. Therefore, they have developed many techniques to measure the initiation of stickiness in powder.

During spray drying, the liquid drop is dried by the surface and its viscosity increases gradually until reaching a possible sticky state. Surface stickiness of the droplet depends on surface temperature, water content and presence of some components in relation with their glass transition temperature. When the particle surface reaches stickiness, collisions with other particles could lead to agglomeration. Agglomeration can be divided into two types which are force agglomeration or desired agglomeration and natural agglomeration or the undesired agglomeration. Force agglomeration is operated in order to improve instant properties such as wettability, dispersability, and solubility of the final dry powder which are required in pharmaceuticals, foods, chemical producing industries. Agglomeration step often follow the simple spray drying. This process will enlarge particle size and it could be performed either outside the drying chamber in an external fluid bed or integrated in the spray drying process. In fluid bed, the already dried particles are rewetted on

surface by sprayed water or other binder solution while in the case of agglomeration occur inside spray drying chamber dried fine particles from cyclones are reintroduced into the drying chamber in the close proximity of the atomizer. The wet concentrate droplets collide with the fines and stick together, forming larger irregular shaped agglomerates.For the natural agglomeration, it can occur during spray drying process. The dry fine particles are not reintroduced into spray chamber. However, the natural agglomeration may appear during storage and is called caking.

Williams *et al.* (2009) studied the effect of fines on agglomeration in spray dryers. The skim milk powder was tested for this effect. The agglomeration efficiency was developed based on examining the agglomerated product size distribution relative to the spray and fines. This efficiency reflects the proportion of particle sizes that disappear from the spray size distribution and then appear in the agglomerated product. They did the experiment and compared the results between the reference case of natural agglomeration when the dryer was run without fines, and later forced agglomeration trials with fines. The results confirm that fines addition does promote agglomeration. Moreover, they found that the concentration of the spray liquid has a weaker effect on influencing forced agglomeration but has a major influence on the particle size of the final product because high solids concentration promote natural agglomeration when sprays interact. This relates to the development of surface stickiness which influences the success of collisions.

2.5 Glass transition temperature

Glass transition temperature (T_g) is the most important descriptor of the properties of amorphous polymers. It is the temperature at which the amorphous phase is converted between rubbery and glassy states. A substance below its T_g is said to be in the glassy state. As the temperature increases, it passes through T_g, and its mechanical properties change from glass to rubber.

The glass transition temperature of a solid–water mixture is strongly dependant on the water concentration, that is, $T_g = f(X_w)$. Once the distribution of

moisture (X_w) within a droplet is known, the distribution of T_g within the droplet can be determined using the Gordon–Taylor equation (Roos, 2002) which is re-written in terms of moisture (X_w) and is given by Equation 10

$$T_g(x_w) = \frac{T_{g,s} + KT_{g,w}x_w}{1 + Kx_w} \quad (1)$$

Where K is the solid–water binary constant that is to be determined experimentally.

2.6 Sticky point temperature

Sticky point temperature is used to predict if the surface of the material is sticky or not. It is based on the fact that for a given combination of material temperature and moisture content, the mass of a powdery material resists movement and is no longer free-flowing. At sticky point temperature, the powder particles show the highest tendency to stick to equipment surfaces or each other.

The sticky point temperature can also be measures or determined through the changes in the mechanical and thermal property of the materials, for example, when the solid state is changed to rubbery state or a low heat capacity solid state transformed into high heat capacity liquid state. Normally, sticky point temperature of the material is found from the experiment. Many techniques were developed to measure this temperature which makes different in definition of sticky point temperature such as from stirrer-type devices, it is defined as the temperature at which the force necessary to turn an impeller in a material sample with defined moisture content increases dramatically. In terms of conventional measurement, sticky point temperature is the temperature at which the bulk mass of a particulate product offers maximum resistance to a shearing motion (Roos, 2002).

3 Computational Fluid Dynamics

Computational Fluid Dynamics (CFD) is a technique that is used to determine the numerical solution for describing the system of fluid flow, heat and mass transfer, and associated phenomena by mean of computer-based simulation (Versteeg, 1995).The physical aspects of any fluid flow are governed by three fundamental principles: Mass is conserved, Newton's second law is conserved and Energy is conserved. These fundamental principles can be expressed in terms of mathematical equations. The set of equations that describe the processes of momentum, heat and mass transfer are known as the Navier-Stokes equations, which are partial differential equations. They are cannot be solved to obtain the general analytical solution but they can be discretised and solved numerically. In CFD technique, the flow region is divided into a large number of finite volumes or cells. The governing partial differential equations are discretised using a wide range of techniques such as finite difference, finite volume or finite element. Each technique has its own mathematical basis but deal with the same fundamental physical relationships of fluid flow. The most common is known as the finite volume method.

Kieviet *et al*. (1997) study to develop a theoretical drying model that would predict the quality of the final product. The study encompassed both measurements and modeling of the air pattern and the temperature and humidity flow fields. The flow fields were simulated using the CFD package FLOW3D^{TM}, body-fitted version 3.3. The spray dryer was a cylinder-on-cone 2.215m diameter, 3.73 m high, dryer fitted with a centrifugal pressure nozzle. Two cases were considered: one with and the other without liquid spray injection. For simulations without spray, swirl was not considered, and the air flow pattern was compared with that obtained with the measured data. The swirl angle was set at 2 □ for the case of droplet spraying, and the experimentally determined temperature and humidity profiles were compared with the profiles predicted by simulations. The flow field was considered to be in steady-state, and time-averaged Navier-Stokes equations were solved applying the k - ε turbulence model. The droplet drying kinetics was assumed to be the same as this for drying pure water droplets. Mass transfer was calculated by using standard mass

transfer correlations, and the Antoine equation was used for estimation of the vapor pressure as a function of temperature. The model took into account the buoyancy of the air due to temperature and humidity differences and heat loss through the chamber walls (however, no information was given about the value of heat transfer coefficient). The model was validated by comparing the predicted results with those obtained by measurements, and a good qualitative agreement was obtained.

Huang *et al*. (2003) study to used a CFD technique for investigating the flow characteristics inside a spray dryer. The spray drying model, incorporated in FLUENT 6.0 was adopted for simulation of the drying process in a cylinder-on-cone drying chamber fitted with a pressure nozzle. The air flow was co-current, and a steady-state, two-dimensional, and axis symmetric flow pattern was assumed. A pressure nozzle located at the top of the chamber was used to atomize a liquid into a spray. A discrete phase model (DPM) was used for tracking the particles trajectories inside the drying chamber (the DPM incorporated in FLUENT is similar to the PSI-cell method). Two-way coupling of heat, mass, and momentum transfer between the continuous and discrete phases was assumed. All particles were considered to ‘‘escape’’ from the calculations when the hitting walls of the drying chamber.

Kieviet and Kerkhof (1997) study to facilitate comparisons the experimental results with FLUENT simulations. The spray of droplets was assumed to have a solids content of 42.5%, and the spray angle was set at 76 □. Droplet distribution was modeled using the Rosin-Rammler distribution, and 20 streams of droplet diameters were tracked. Droplet drying kinetics was simplified by assuming the physical properties of the feed to be similar to those of the water, with the exception that the volatile content changed as the drying proceeded. The effects of turbulence were considered by the standard k - ε turbulence model. The results of the simulations for velocity, temperature, and humidity profiles at different chamber levels showed good agreement with published experimental data.

Mezhericher *et al*. (2010a) study was to model the process of droplet drying in the spray chamber using CFD techniques and to perform 2D axisymmetric and 3D

numerical simulations of heat and mass transfer in the chamber. Based on the results of steady-state and unsteady-state computations, either a 2D or 3D model can be recommended for practical utilization in the specific cases.

Mezhericher *et al*. (2010b) study was to conduct a computational study of the influence of droplet–droplet interactions on the process of spray drying in 2D coordinate space. For this purpose, a theoretical model of the two-phase flow, based on a Eulerian approach for the continuous phase (drying agent) and a Lagrangian approach for the discrete phase (spray of droplets), was developed. Droplet-droplet interactions were treated by the probabilistic approach developed by O'Rourke. For numerical solution of the developed model and computational simulations, the CFD package FLUENT 6.3.26 was utilized.

Mezhericher *et al*. (2010c) study was to develop a two-dimensional theoretical model of the steady-state spray drying process incorporating a comprehensive description of two-stage droplet drying kinetics. Such a model can be regarded as a first approximation to realistic theoretical modelling of the actually three-dimensional and unsteady spray drying process.

3.1 Finite Volume Method

This finite volume technique is most popular method because this technique can accommodate any type of grid, thus it is appropriate for complex geometries. The grid defines only the control volume boundaries and need not be related to a coordinate system. The finite volume approach is perhaps the simplest to understand and program. Moreover, in this technique, all terms that need to be approximated have physical meaning. The region of interest is divided into small sub-regions, called control volumes. The equations are discretised and solved iteratively for each control volume. Values of the solution variables are obtained at the elements or cells, and there is usually at least one equation for each variable at each element or cell. As a result, an approximation of the value of each variable at specific points throughout the domain can be obtained. In this way, a full picture of the behavior of the flow can be derived.

3.2 Structure of CFD Code

CFD codes are structured around the numerical algorithms that can tackle fluid flow problems. In order to provide easy access to their solving power all commercial CFD packages include sophisticated user interfaces to input problem parameters and to examine the results. Hence all codes contain three main elements: (1) a pre-processor, (2) a solver and (3) a post-processor.

Pre-processor

Pre-processor consists of the input of a flow problem to a CFD program by means of an operator-friendly interface and the subsequent transformation of this input into a form suitable for use by the solver. The user activities at the pre-processing stage involve:

- Definition of the geometry of the region of interest: the computational domain
- Grid generation the sub-division of the domain into a number of smaller, non-overlapping sub-domains: a grid (or mesh) of cells (or control volumes or elements)
- Selection of the physical and chemical phenomena that need to be modeled.
- Definition of fluid properties.
- Specification of appropriate boundary conditions at cells which coincide with or touch the domain boundary.

The solution of a flow problem (velocity, pressure, temperature etc.) is defined at nodes inside each cell. The accuracy of a CFD solution is governed by the number of cells in the grid. In general, the larger number of cells the better the accuracy of the solution. Both the accuracy of a solution and its cost in terms of necessary computer hardware and calculation time are dependent on the fineness of the grid. Optimal meshes are often non-uniform: finer in areas where large variations occur from point to point and coarser in regions with relatively little change. Efforts are under way to develop CFD codes with a self-adaptive meshing capability. Ultimately such amount

of basic development work still needs to be done before these techniques are robust enough to be incorporated into commercial CFD codes. At present it is still up to the skills of the CFD user to design a grid that is a suitable compromise between desired accuracy and solution cost. Over 50% of the time spent in industry on a CFD project is devoted to the definition of the domain geometry and grid generation. In order to maximize productivity of CFD personnel all the major codes now include their own CAD-style interface and or facilities to import data from proprietary surface modelers and mesh generators such as PATRAN and I-DEAS. Up to date pre-processors also give the user access to libraries of material properties for common fluids and a facility to invoke special physical and chemical process models (e.g. turbulence models, radiation heat transfer, combustion models) alongside the main fluid flow equations.

Solver

There are many distinct streams of numerical solution techniques. In outline the numerical methods that form the basis of the solver perform the following steps:

- Approximation of the unknown flow variables by means of simple functions.
- Discretization by substitution of the approximations into the governing flow equations and subsequent mathematical manipulations.
- Solution of the algebraic equations.

The main differences between the three separated streams are associated with the way in which the flow variables are approximated and with the discretization processes.

Post-processor

As in pre-processing a huge amount of development work has recently taken place in the post-processing field. Owing to the increased popularity of engineering workstations, many of which have outstanding graphics capabilities, the leading CFD packages are now equipped with versatile data visualization tools. These include:

- Domain geometry and grid display
- Vector plots
- Line and shaded contour plots

- 2D and 3D surface plots
- Particle tracking
- View manipulation (translation, rotation, scaling etc.)
- Color postscript output

3.3 Fluent Software

Fluent is the leading supplier of computational fluid dynamics (CFD) software and service. Fluent has significant expertise in the core areas of turbulence modeling, high performance computing and algorithm development, as well as in challenging applications in the power generation and chemical and process industries, safety, and the environment. Fluent is a finite volume based CFD code, combining an advanced solver with powerful pre- and post-processing capabilities. The process of performing a single CFD simulation is split into four components that shown as following.

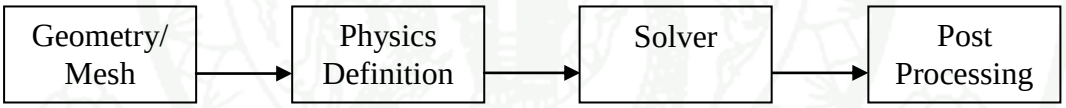

Figure 5 The processing component in Fluent software

Fluent uses a coupled solver, which solves the hydrodynamic equations as a single system. This solution approach uses a fully implicit discretization of the equations at any given time step. For steady state problems the time-step behaves like an acceleration parameter, to guide the approximate solutions in a physically based manner to a steady state solution. This reduces the number of iterations required for convergence to a steady state, or to calculate the solution for each time step in a time dependent analysis. More recently these facilities may also include animation for dynamic result display and in addition to graphics all codes produce trusty alphanumeric output and have data export facilities for further manipulation external to the code. As in many other branches of Computer Aided Engineering (CAE) the graphics output capabilities of CFD codes have revolutionized the communication of

ideas to the non-specialist. Nowadays, there is several CFD related software available in the software market all over the world such as SOLID WORK , ANSYS version 12.1 , and FLUENT. In this research, FLUENT version 6.3 will be used extensively.

3.4 Discrete Phase Modeling (DPM)

In addition to solving transport equations for the continuous phase, FLUENT allows you to simulate a discrete second phase in a Lagrangian frame of reference. This second phase consists of spherical particles (which may be taken to represent droplets or bubbles) dispersed in the continuous phase. FLUENT computes the trajectories of these discrete phase entities, as well as heat and mass transfer to/from them. The coupling between the phases and its impact on both the discrete phase trajectories and the continuous phase flow can be included.

FLUENT provides the following discrete phase modeling options:

- calculation of the discrete phase trajectory using a Lagrangian formulation that includes the discrete phase inertia, hydrodynamic drag, and the force of gravity, for both steady and unsteady flows
- prediction of the effects of turbulence on the dispersion of particles due to turbulent eddies present in the continuous phase
- heating/cooling of the discrete phase
- vaporization and boiling of liquid droplets
- combusting particles, including volatile evolution and char combustion to simulate coal combustion
- optional coupling of the continuous phase flow field prediction to the discrete phase calculations
- droplet breakup and coalescence These modeling capabilities allow FLUENT to simulate a wide range of discrete phase problems including particle separation and classification, spray drying, aerosol dispersion, bubble stirring of liquids, liquid fuel combustion, and coal combustion.

The fluid phase is treated as a continuum by solving the time-averaged Navier-Stokes equations, while the dispersed phase is solved by tracking a large number of

particles, bubbles, or droplets through the calculated flow field. The dispersed phase can exchange momentum, mass, and energy with the fluid phase. A fundamental assumption made in this model is that the dispersed second phase occupies a flow volume fraction, even though high mass loading ($m_{particles} \geq m_{fluid}$) is acceptable.

The particle or droplet trajectories are computed individually at specified intervals during the fluid phase calculation. This makes the model appropriate for the modeling of spray dryers, coal and liquid fuel combustion, and some particle-laden flows, but inappropriate for the modeling of liquid-liquid mixtures, fluidized beds, or any application where the volume fraction of the second phase is not negligible.

3.4.1 Setting Initial Conditions for the Discrete Phase

For liquid sprays, a convenient representation of the droplet size distribution is the Rosin- Rammler expression. The complete range of sizes is divided into an adequate number of discrete intervals; each represented by a mean diameter for which trajectory calculations are performed. If the size distribution is of the Rosin-Rammler type, the mass fraction of droplets of diameter greater than d is given by:

$$Y_d = e^{-(d/\bar{d})^n} \qquad (2)$$

where $\bar{d}$ is the size constant and n is the size distribution parameter (n=2.09). Use of the Rosin- Rammler size distribution of particles by inputting a diameter for the first and last points to vary the diameter of each particle stream in the group.When you want a different mass flow rate for each particle/droplet size, however, the linear variation may not yield the distribution you need. Your particle size distribution may be defined most easily by fitting the size distribution data to the Rosin-Rammler equation. In this approach, the complete range of particle sizes is divided into a set of discrete size ranges, each to be defined by a single stream that is part of the group. Assume, for example, that the particle size data obeys the following distribution:

Table 1 The Rosin-Rammler distribution

Diameter Range (μm)	Mass Fraction in Range (s)
0-70	0.05
70-100	0.10
100-120	0.35
120-150	0.30
150-180	0.15
180-200	0.05

The Rosin-Rammler distribution function is based on the assumption that an exponential relationship exists between the droplet diameter, d, and the mass fraction of droplets with diameter greater than d, Y_d : FLUENT refers to the quantity $\bar{d}$ in Equation 2 the Mean Diameter and to n as the Spread Parameter. These parameters are input by you (in the Set Injection Properties panel under the First Point heading) to define the Rosin-Rammler size distribution. To solve for these parameters, you must fit your particle size data to the Rosin-Rammler exponential equation. To determine these inputs, first recast the given droplet size data in terms of the Rosin-Rammler format. For the example data provided above, this yields the following pairs of d and Y_d:

Table 2 The Mass fraction of droplets with sizes larger than d

Diameter Range (μm)	Mass Fraction with Diameter Greater than d, Y_d
70	0.95
100	0.85
120	0.50
150	0.20
180	0.05
200	0.00

A plot of Y_d vs. d is shown in Figure 6

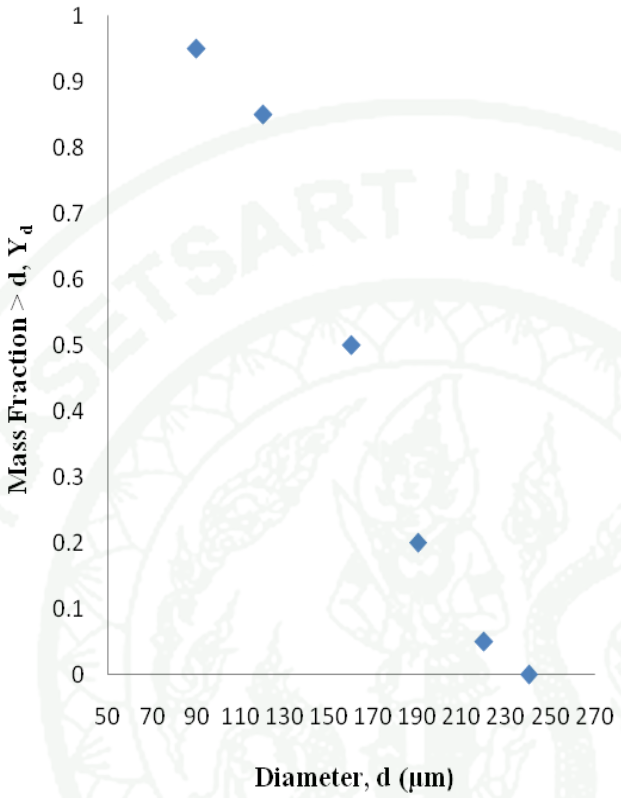

Figure 6 The Size Distribution of Particles

Source: Fluent Manual (2010)

This technique of fitting the Rosin-Rammler curve to spray data is used when reporting the Rosin-Rammler diameter and spread parameter in the discrete phase.

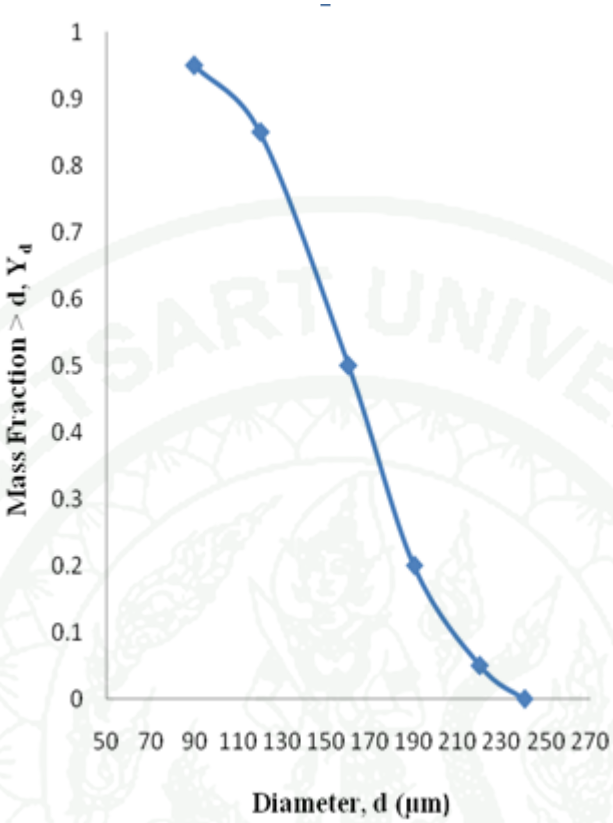

Figure 7 Rosin-Rammler Curve Fit for the Particle Size Data

Source: Fluent Manual (2010)

A second Rosin-Rammler distribution is also available based on the natural logarithm of the particle diameter. If in your case, the smaller-diameter particles in a Rosin-Rammler distribution have higher mass flows in comparison with the larger-diameter particles, you may want better resolution of the smaller-diameter particle streams, or "bins" You can therefore choose to have the diameter increments in the Rosin-Rammler distribution done uniformly by ln d. In the standard Rosin-Rammler distribution, a particle injection may have a diameter range of 1 to 200 μm. In the logarithmic Rosin-Rammler distribution, the same diameter range would be converted to a range of ln 1 to ln 200, or about 0 to 5.3. In this way, the mass flow in one bin would be less-heavily skewed as compared to the other bins.

3.4.2 Setting Boundary Conditions for the Discrete Phase

When a particle reaches a physical boundary (e.g., a wall or inlet boundary) in your model, FLUENT applies a discrete phase boundary condition to determine the fate of the trajectory at that boundary. The boundary condition, or trajectory fate, can be defined separately for each zone in your FLUENT model. Discrete Phase Boundary Condition Types. The available boundary conditions include the following:

- "Refect" the particle rebounds of the boundary in question with a change in its momentum as defined by the coefficient of restitution.

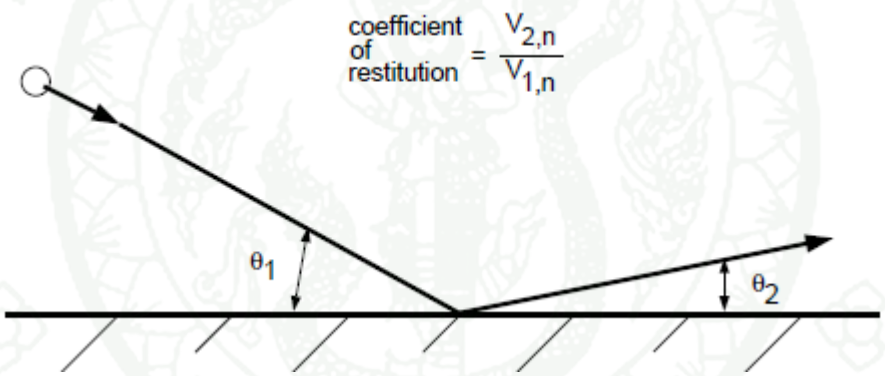

Figure 8 "Refect" Boundary Condition for the Discrete Phase

Source: Fluent Manual (2010)

- "Trap" the trajectory calculations are terminated and the fate of the particle is recorded as"trapped". In the case of evaporating droplets, their entire mass instantaneously passes into the vapor phase and enters the cell adjacent to the boundary. See Figure 9 In the case of combusting particles, the remaining volatile mass is passed into the vapor phase.

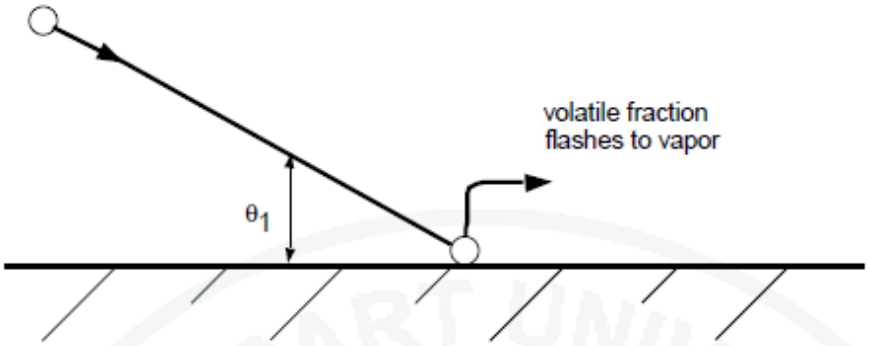

Figure 9 "Trap" Boundary Condition for the Discrete Phase

Source: Fluent Manual (2010)

- "Escape" the particle is reported as having "escaped" when it encounters the boundary in question. Trajectory calculations are terminated.

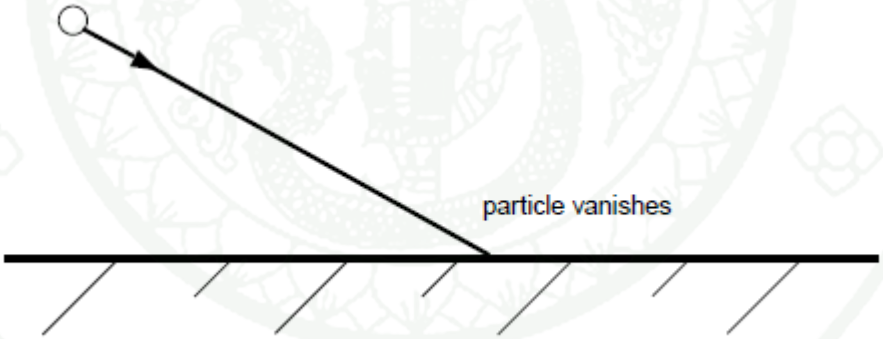

Figure 10 "Escape" Boundary Condition for the Discrete Phase

Source: Fluent Manual (2010)

3.5 Particle Motion Theory

Equations of Motion for Particles FLUENT predicts the trajectory of a discrete phase particle (or droplet or bubble) by integrating the force balance on the particle, which is written in a lagrangian reference frame. This force balance equates the particle inertia with the forces acting on the particle, and can be written (for the x direction in Cartesian coordinates) as

$$\frac{du_p}{dt} = F_D\left(u - u_p\right) + \frac{g_x\left(\rho_p - \rho\right)}{\rho_p} + F_x \tag{3}$$

where F_x is an additional acceleration (force/unit particle mass) term, $F_D\,(u-u_p)$ is the drag force per unit particle mass and

$$F_D = \frac{18\mu}{\rho_p d_p^2}\frac{C_D\,\mathrm{Re}}{24} \tag{4}$$

Here, u is the fluid phase velocity, u_p is the particle velocity, μ is the molecular viscosity of the fluid, p is the fluid density, p_p is the density of the particle, and d_p is the particle diameter. Re is the relative Reynolds number, which is defined as

$$\mathrm{Re} \equiv \frac{\rho d_p \left|u_p - u\right|}{\mu} \tag{5}$$

3.6 Spray Model Theory

In addition to the simple injection types FLUENT also provides more complex injection types for sprays. For most types of injections, you will need to provide the initial diameter, position, and velocity of the particles. For sprays, however, there are models available to predict the droplet size and velocity distributions. Models are also available for droplet breakup and collision, as well as a dynamically varying drag coefficient which accounts for variation in droplet shape.

These models for realistic spray simulations are described in this section. Information is organized into the following subsections:

3.6.1 Droplet Collision Model

When your simulation includes tracking of droplets, FLUENT provides an option for estimating the number of droplet collisions and their outcomes in a computationally efficient manner. The difficulty in any collision calculation is that for N droplets, each droplet has N - 1 possible collision partners. Thus, the number of possible collision pairs is approximately $1/2N_2$. (The factor of $1/2$ appears because droplet A colliding with droplet B is identical to droplet B colliding with droplet A. This symmetry reduces the number of possible collision events by half.) An important consideration is that the collision algorithm must calculate $1/2N_2$ possible collision events at every time step. Since a spray can consist of several million droplets, the computational cost of a collision calculation from first principles is prohibitive. This motivates the concept of parcels. Parcels are statistical representations of a number of individual droplets. For example, if FLUENT tracks a set of parcels, each of which represents 1000 droplets, the cost of the collision calculation is reduced by a factor of 10^6. Because the cost of the collision calculation still scales with the square of N the reduction of cost is significant; however, the effort to calculate the possible intersection of so many parcel trajectories would still be prohibitively expensive. The collision model assumes that the frequency of collisions is much less than the particle time step. If the particle time step is too large, then the results may be time step-dependent. You should adjust the particle length scale accordingly. Additionally, the model is most applicable for low-Weber-number collisions where collisions result in bouncing and coalescence. Above a Weber number of about 100, the outcome of collision could be shattering. Sometimes the collision model can cause grid-dependent artifacts to appear in the spray. This is a result of the assumption that droplets can collide only within the same cell. These tend to be visible when the source of injection is at a mesh vertex. The coalescence of droplets tends to cause the spray to pull away from cell boundaries. In two dimensions, a finer mesh and more computational droplets can be used to reduce these

effects. In three dimensions, best results are achieved when the spray is modeled using a polar mesh with the spray at the center.

If the collision model is used in a transient simulation, multiple DPM iterations per time step cannot be specified in the Number of Continuous Phase Iterations per DPM Iteration field in the Discrete Phase Model panel. In such cases, only one DPM iteration per time step will be calculated. As noted above, O'Rourke's algorithm assumes that two droplets may collide only if they are in the same continuous-phase cell. This assumption can prevent droplets that are quite close to each other, but not in the same cell, from colliding, although the effect of this error is lessened by allowing some droplets that are farther apart to collide. The overall accuracy of the scheme is second-order in space.

3.6.2 Droplet Breakup Models

FLUENT offers two droplet breakup models: the Taylor analogy breakup (TAB) model and the wave model. The TAB model is recommended for low-Weber-number injections and is well suited for low-speed sprays into a standard atmosphere. For Weber numbers greater than 100 the wave model is more applicable. The wave model is popular for use in high-speed fuel-injection applications. Details for each model are provided below. The resulting TAB model equation set which governs the oscillating and distorting droplet, can be solved to determine the droplet oscillation and distortion at any given time. As described in detail below, when the droplet oscillations grow to a critical value the parent droplet will break up into a number of smaller child droplets. As a droplet is distorted from a spherical shape the drag coefficient changes. A drag model that incorporates the distorting droplet effects is available in FLUENT.

3.7 Atomizer Model Theory

Atomization models use physical atomizer parameters, such as orifice diameter and mass flow rate, to calculate initial droplet size, velocity, and position.For realistic atomizer simulations, the droplets must be randomly distributed, both

spatially through a dispersion angle and in their time of release. For other types of injections in FLUENT (nonatomizer), all of the droplets are released along fixed trajectories at the beginning of the time step. The atomizer models use stochastic trajectory selection and staggering to attain a random distribution.Stochastic trajectory selection is the random dispersion of initial droplet directions. All of the atomizer models provide an initial dispersion angle, and the stochastic trajectory selection picks an initial direction within this angle. This approach improves the accuracy of the results for spray-dominated flows. The droplets will be more evenly spread among the computational cells near the atomizer, which improves the coupling to the gas phase by spreading drag more smoothly over the cells near the injection. Source terms in the energy and species conservation equations are also more evenly distributed among neighboring cells improving solution convergence. Five atomizer models are available in FLUENT to predict the spray characteristics from knowledge of global parameters such as nozzle type and liquid flow rate.

- plain-orifice atomizer
- pressure-swirl atomizer
- at-fan atomizer
- air-blast/air-assisted atomizer
- effervescent/flashing atomizer

Can choose them as injection types and define the associated parameters in the Set Injection Properties panel.

The atomisation stage during spray drying is very important since it affects the final particle size. A co-current spray-dryer fitted with pressure nozzle was investigated both in experiment and CFD simulation by (Kieviet and Kerkhof, 1997) to develop a theoretical model for the prediction of final product quality. Good agreement was obtained between the experimental data and the simulation.

3.8 One-Way and Two-Way Coupling

FLUENT to predict the discrete phase patterns based on a fixed continuous phase flow field (an uncoupled approach or one-way coupling), or you can include the effect of the discrete phase on the continuum (a coupled approach or two-way coupling). In the coupled approach, the continuous phase flow pattern is impacted by the discrete phase (and vice versa), and you can alternate calculations of the continuous phase and discrete phase equations until a converged coupled solution is achieved. FLUENT's discrete phase modeling capability, reacting particles or droplets can be modeled and their impact on the continuous phase can be examined. Several heat and mass transfer relationships, termed laws, are available in FLUENT and the physical models employed in these laws are described in this section.

3.8.1 Coupling Between the Discrete and Continuous Phases

As the trajectory of a particle is computed, FLUENT keeps track of the heat, mass,and momentum gained or lost by the particle stream that follows that trajectory and these quantities can be incorporated in the subsequent continuous phase calculations. Thus, while the continuous phase always impacts the discrete phase, you can also incorporate the effect of the discrete phase trajectories on the continuum. This two-way coupling is accomplished by alternately solving the discrete and continuous phase equations until the solutions in both phases have stopped changing. This interphase exchange of heat, mass, and momentum from the particle to the continuous phase is depicted qualitatively in Figure 11

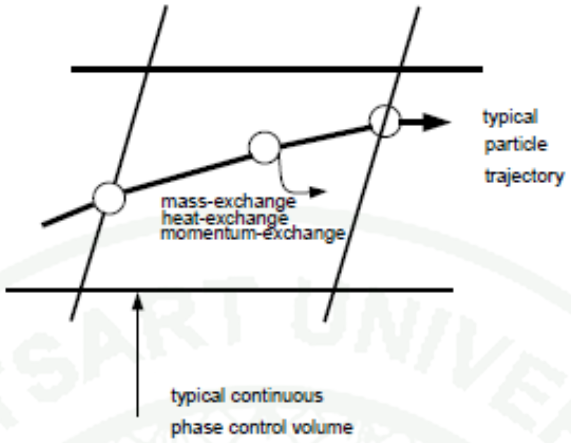

Figure 11 Heat, Mass, and Momentum Transfer Between the Discreteand Continuous Phases

Source: Modeling Discrete Phase (2009).

Momentum Exchange

The momentum transfer from the continuous phase to the discrete phase is computed in FLUENT by examining the change in momentum of a particle as it passes through each control volume in the FLUENT model. This momentum change is computed as

$$F = \sum \left(\frac{18\mu C_D \,\mathrm{Re}}{\rho_p d_p^2 24} \left(u_p - u \right) + F_{other} \right) \dot{m}_p \Delta t \qquad (6)$$

where

μ = viscosity of the fluid

ρ_p = density of the particle

d_p = diameter of the particle

Re = relative Reynolds number

u_p = velocity of the particle

u = velocity of the fluid

C_D = drag coefficient

$\dot{m}_p$ = mass flow rate of the particles

Δt = time step

F_{other} = other interaction forces

This momentum exchange appears as a momentum sink in the continuous phase momentum balance in any subsequent calculations of the continuous phase flow field and can be reported by FLUENT as described.

Heat Exchange

The heat transfer from the continuous phase to the discrete phase is computed in FLUENT by examining the change in thermal energy of a particle as it passes through each control volume in the FLUENT model. The heat exchange is computed as

$$Q = \left(m_{p_{in}} - m_{p_{out}}\right)\left[-H_{latref} + H_{pyrol}\right] - m_{p_{out}}\int_{T_{ref}}^{T_{p_{out}}} c_{p_p}\,dT + m_{p_{in}}\int_{T_{ref}}^{T_{p_{in}}} c_{p_p}\,dT \quad (7)$$

where

$m_{p_{in}}$ = mass of the particle on cell entry (kg)

$m_{p_{out}}$ = mass of the particle on cell exit (kg)

c_{p_p} = heat capacity of the particle (J/kg-K)

H_{pyrol} = heat of pyrolysis as volatiles are evolved (J/kg)

$T_{p_{in}}$ = temperature of the particle on cell entry (K)

$T_{p_{out}}$ = temperature of the particle on cell exit (K)

T_{ref} = reference temperature for enthalpy (K)

H_{latref} = latent heat at reference conditions (J/kg)

The latent heat at the reference conditions H_{latref} for droplet particles is computed as the difference of the liquid and gas standard formation enthalpies, and can be related to the latent heat at the boiling point as follows:

$$H_{lat_{ref}} = H_{lat} - \int_{T_{ref}}^{T_{p,init}} c_{p_g} dT + \int_{T_{ref}}^{T_{p,init}} c_{p_p} dT \quad (8)$$

where

$T_{p,init}$ = particle initial temperature (K)

T_{ref} = particle reference temperature (K)

$H_{lat_{ref}}$ = latent heat at the reference conditions

H_{lat} = latent heat

Mass Exchange

The mass transfer from the discrete phase to the continuous phase is computed in FLUENT by examining the change in mass of a particle as it passes through each control volume in the FLUENT model. The mass change is computed simply as

$$M = \frac{\Delta m_p}{m_{p,0}} \dot{m}_{p,0} \quad (9)$$

This mass exchange appears as a source of mass in the continuous phase continuity equation and as a source of a chemical species defined by you. The mass sources are included in any subsequent calculations of the continuous phase flow field and are reported by FLUENT.

3.9 Air flow pattern

During spray drying the particle behaviour is dependent on the air flow pattern. Earlier studies were based on the semi-empirical models for understanding of the spray-drying process. Inside the spray chamber there is presence of significant air

flow instabilities due to the inlet swirl. Hence, the effect of turbulence inside the spray chamber should be considered.

3.9.1 Turbulence models

Most commercial CFD codes use turbulence models that are based on the splitting up of instantaneous quantities into a time-averaged and a fluctuating part by a process known as Reynolds decomposition. Four turbulence models are commonly used for simulating sprays: (i) standard k- ε (k-ε turbulence kinetic energy and k-ε turbulence dissipation rate) (ii) RNG k -ε, (iii) realizable k -ε, (iv) Reynolds Stress Model (RSM).

Three models (standard, RNG, and realizable k -ε) have similar forms, with transport equations for k and ε. The standard k -ε model focuses on the mechanisms that affect the turbulent kinetic energy. It can be used over a wide range of turbulent flows due to its robustness and reasonable accuracy. In the realizable k -ε model, the term "realizable" means that the model satisfies certain mathematical constraints on the normal stresses, consistent with the physics of turbulent flows. It provides better prediction for flows involving rotation, boundary layers under strong adverse pressure gradients, separation, and recirculation (Anderson, 1984)

The RNG-based k -ε turbulence model is derived from the instantaneous NaviereStokes equations, using a mathematical technique called "renormalization group" (RNG) methods. The analytical derivation results in a model with constants different from those in the standard k -ε model and additional terms and functions in the transport equations for k and ε. The effect of swirl on turbulence is included in the RNG model, which enhancing accuracy for swirling flows.

The Reynolds Stress Model has the same general form as the instantaneous NaviereStokes equations, with the velocities and other solution variables ensemble-averaged (or time-averaged). The RSM is clearly superior for problems where anisotropy of turbulence has a dominant effect on the mean flow

(e.g. highly swirling flows) (Bakker, 2002). For turbulent flows, the standard ke3 model (k - ε turbulence kinetic energy and k - ε turbulence dissipation rate) is themost commonly used, because it converges considerably better than Reynolds stress model (RSM). The standard k - ε turbulence model is used commonly where there is no swirling flow. The transport of the turbulence kinetic energy k and its dissipation rate ε is given as follows:

$$\frac{\partial}{\partial t}(\rho k) + \nabla.(\rho k \underline{v}) = \nabla.\left[\left(\mu + \frac{\mu_t}{\sigma_k}\right)\nabla k\right] + G_k - \rho\varepsilon \tag{10}$$

and

$$\frac{\partial}{\partial t}(\rho \varepsilon) + \nabla.(\rho \varepsilon \underline{v}) = \nabla.\left[\left(\mu + \frac{\mu_t}{\sigma_\varepsilon}\right)\nabla \varepsilon\right] + C_{1\varepsilon}\frac{\varepsilon}{k}(G_k) - C_{2\varepsilon}\rho\frac{\varepsilon^2}{k} \tag{11}$$

G_k is the generation of kinetic energy due to the mean velocity gradients. The quantities σ_k and σ_ε are the turbulent Prandtl numbers for k and ε, respectively and $C_{1\varepsilon}$, $C_{2\varepsilon}$, are constant. The turbulent (or eddy) viscosity, μ_t is calculated from k and ε as follows

$$\mu_t = \rho C_\mu \frac{k^2}{\varepsilon} \tag{12}$$

For calculating an approximate solution of fluid flow equations, the equations have to be made discrete. For this, the flow domain is divided into number of control volumes. This is called a grid and at each grid cell approximate solutions for the Navier-Stokes and the continuity equations are calculated.

MATERIALS AND METHODS

Materials

1. Personal Computer (PC)
   - CPU (Intel(R) Pentium(R) D CPU 3.40 GHz (2CPUs))
   - 2.00 GB of RAM
   - 240 GB of hard disk
2. Operating System: Microsoft Window XP Professional 2002 service pack 2
3. Soft wares
   - SOLID WORK version 2010
   - ANSYS version 12.1
   - FLUENT version 6.3

Methods

This work considers the spray drying model for prediction the effects internal behavior of the spray dryer in milk powder displace the region of heat and mass transfer from the central core toward the periphery of the drying chamber. In this work, The spray drying model was divided into four major parts. The first part is the model to validated with the experiment data of Kieveit (1997) for the accuracy of the model. The second part was the model to predict the air flow pattern. The third part, the model predict the particle residence time distribution. Next, the model to predict occurrence of stickiness in the spray drying. The methodology that is used to accomplish this thesis consists of 5 steps as shown in Figure 12.

The procedures of the work are

1. Study theory and review literatures that relate to spray drying simulation.
2. Formulate spray drying model for prediction stickiness on the process of spray drying.
3. Generated the geometry for the simulation by SOLID WORK v. 2010

4. Generated mesh for the simulation by ANSYS WORKBENCH v. 12.1
5. Simulating for spray model by FLUENT v. 6.3

1. Study theory and review literatures that relate to spray drying simulation

In the beginning, all the information that relate to the effects internal behavior of the spray dryer in milk powder from the internet, handbook, and literature. The overview of these phenomena is studied including literature review by specified especially on the spray drying model. All the information is analyzed for first understanding about what the stickiness and how these phenomena can occur. Moreover, the theories that related to the drying process such as heat and mass transfer, drying kinetics, and the concept of the droplet-droplet interactions are studied to understand the concept of the velocity, temperature profile of skim milk powder. From all of the literatures that are reviewed, the spray drying model of this thesis is divided into 4 parts as shown below.

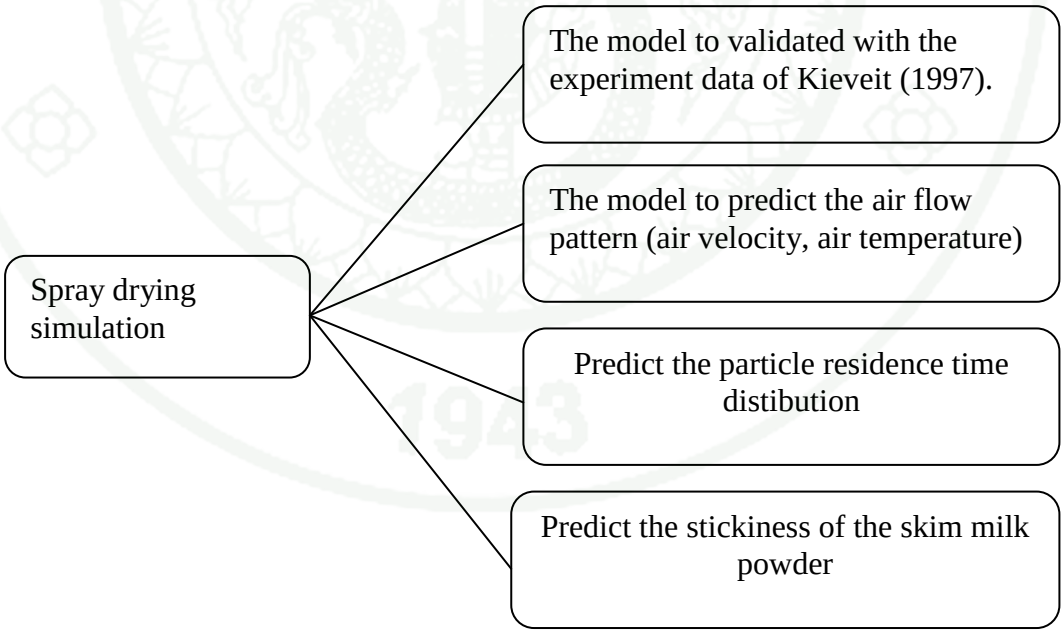

Figure 12 The overview of Spray drying simulation of stickiness process in milk powder

2. Formulate spray drying model for prediction stickiness on the process of spray drying

Spray drying simulation

The spray drying simulation combined Eulerian and Lagrangian model is used to obtain particle trajectories by solving the force balance equation:

$$\frac{d\underline{u}_p}{dt} = \frac{18\mu}{p_p d_p}\frac{C_D \,\mathrm{Re}}{24}(\underline{v} - \underline{u}_p) + \underline{g}\left[\frac{\rho_p - \rho_g}{\rho_p}\right] \tag{13}$$

where, $\underline{v}$ is the fluid phase velocity, $\underline{u}_p$ is the particle velocity, ρ_g is the density of the fluid and ρ_p is the density of the particle.

The particle force balance (equation of motion) includes discrete phase inertia, aerodynamic drag and gravity. The slip Reynolds number (Re) and drag coefficient (C_D) are given in the following equations.

$$\mathrm{Re} = \frac{\rho_g d_p \left|\underline{u}_p - \underline{v}\right|}{\mu} \tag{14}$$

$$C_D = a_1 + \frac{a_2}{\mathrm{Re}} + \frac{a_3}{\mathrm{Re}^2} \tag{15}$$

Where d_p is the particle diameter, and a_1, a_2 and a_3 are constants that apply to smooth spherical particles over several ranges of Reynolds number (Re).

The heat and mass transfer between the particles and the hot gas is derived following the motion of the particles.

$$m_p c_p \frac{dT_p}{dt} = hA_p\left(T_g - T_p\right) + \frac{dm_p}{dt}h_{fg} \tag{16}$$

where, m_p is the mass of the particle, c_p is the particle heat capacity, T_p is the particle temperature, h_{fg} is the latent heat, A_p is the surface area of the particle and h is the heat transfer coefficient.

The heat transfer coefficient (h) is obtained from the Ranze-Marshall equation.

$$Nu = \frac{hd_p}{k_{ta}} = 2 + 0.6\left(\mathrm{Re}_d\right)^{1/2}\left(\mathrm{Pr}\right)^{1/3} \tag{17}$$

where, Prandtl number (Pr) is defined as follows

$$\mathrm{Pr} = \frac{c_p \mu}{k_{ta}} \tag{18}$$

where, d_p is the particle diameter, k_{ta} is the thermal conductivity of the fluid, m is the molecular viscosity of the fluid.

The mass transfer rate (for evaporation) between the gas and the particles is calculated from the following equation

$$\frac{dm_p}{dt} = -k_c A_p \left(Y_s - Y_g\right) \tag{19}$$

where, Y_s is the saturation humidity, Y_g is the gas humidity and k_c is the mass transfer coefficient and it can be obtained from Sherwood number.

$$Sh = \frac{k_c d_p}{D_{i,m}} = 2 + 0.6\left(\mathrm{Re}_d\right)^{1/2}\left(Sc\right)^{1/3} \tag{20}$$

where, $D_{i,m}$ is the diffusion coefficient of water vapour in the gas phase and Sc is the Schmidt number, defined as follows

$$Sc = \frac{\mu}{\rho_g D_{i,m}} \tag{21}$$

The values of vapour pressure, density, specific heat and diffusion coefficients can be obtained from various sources like.

When the temperatures of the droplet has reached the boiling point and while the mass of the droplet exceeds the non-volatile fraction. The boiling rate model was applied

$$\frac{d\left(d_p\right)}{dt} = \frac{4k_{ta}}{\rho_p c_g d_p}\left(1+0.23\sqrt{\mathrm{Re}}\right)\ln\left[1+\frac{c_g(T_g-T_p)}{h_{fg}}\right] \tag{22}$$

where, k_{ta} is the thermal conductivity of the gas and c_g is the heat capacity of the gas.

The necessary assumptions are made in order to simplify the model.

1. Spray drying chamber is assumed to cylinder-on-cone.
2. Droplet sprayed from pressure nozzle atomization has hollow cone spray pattern.
3. The air flow pattern inside spray drying camber is co-current.
4. Heat and mass transfer of the droplet come from the drying kinetics for a single droplet.
5. No hygroscopic capillary-porous media in spherical shape is assumed for the particles.
7. Physical properties such as, thermal conductivity, density and viscosity of the gas, mass diffusivity and heat capacity of the particle are constant.
8. The agglomerated powders still have the same spherical shape.
9. Consider effect gravity force.
10. Consider effect droplet – droplet interaction.

The configuration of spray drying chamber and the hollow cone spray pattern are shown in Figure 13 and 14, respectively. As shown in figures 14, the air inlet and pressure nozzle atomization are at the top of spray chamber. For the parameters that are used in the simulation will be shown in Appendix B.

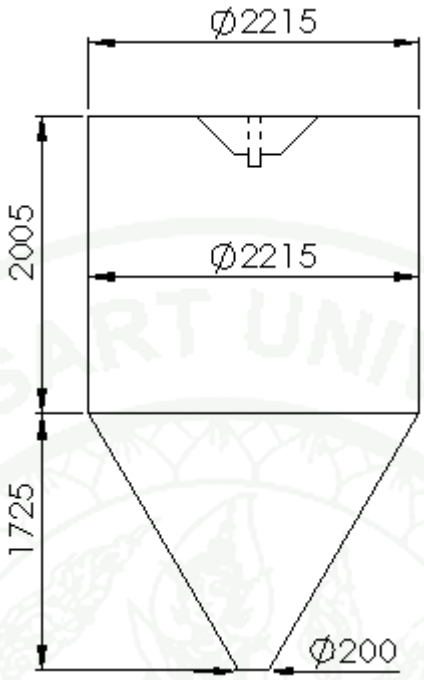

Figure 13 Configuration of spray drying chamber size

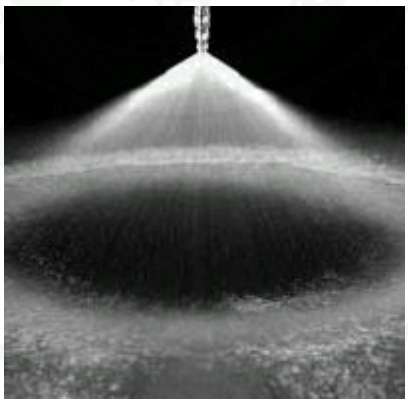

Figure 14 Hollow cone spray pattern photograph

3. Generated the geometry for the simulation by SOLID WORK version 2010

The geometry for the simulation by SOLID WORK shown in Figure 15 and 16 the Figure 15 the dimensions of the chamber and air inlet size are taken as the same as those in the experimental studies of Kieveit (1997) (diameter 2.2 m; height 3.7 m) the Figure 16 the dimensions of the chamber and air inlet size are taken as the same as those in the experimental studies of Kieveit (1997) Part of this work have been added cyclone separator particle from the air. which is located at the top of the chamber. The hot air enters the top of the chamber through an annulus and is evacuated through the pipe in the conical part of the chamber.

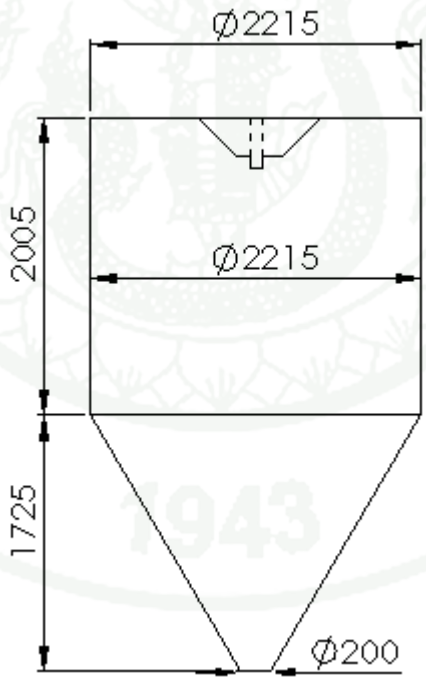

Figure 15 Geometry of the spray dry chamber (mm)

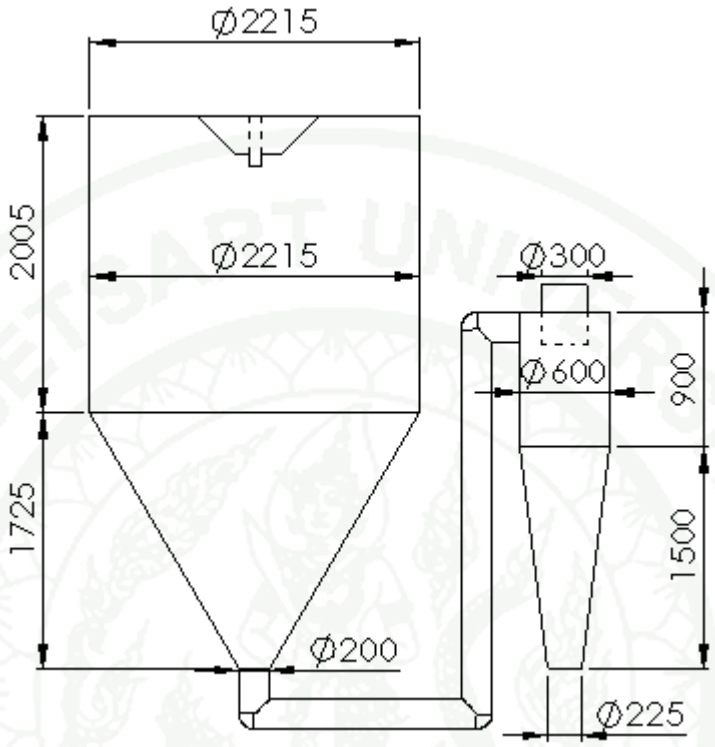

Figure 16 Geometry of the process spray dry (mm)

4. Generated mesh for the simulation by ANSYS WORKBENCH 12.1

The mesh geometry for the simulation by ANSYS WORKBENCH shown in Figure 17 and 18 the Figure 17 have number of grid equal to 120,000 grid and Figure 18 have number of grid equal to 185,000 grid.The method used to generated mesh is unstructure mesh.The program is used to generated mesh.The type of grid is triangle mesh.

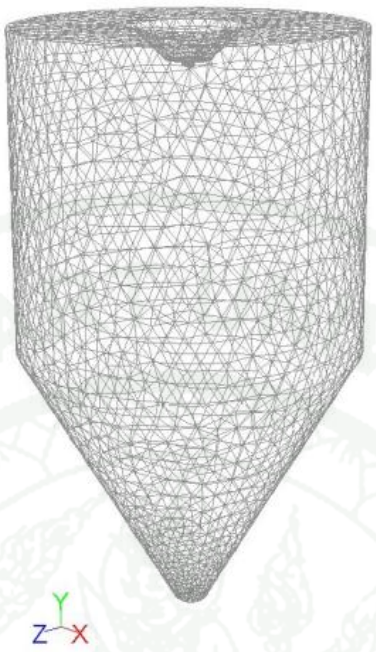

Figure 17 Mesh of the spray dry chamber (mm)

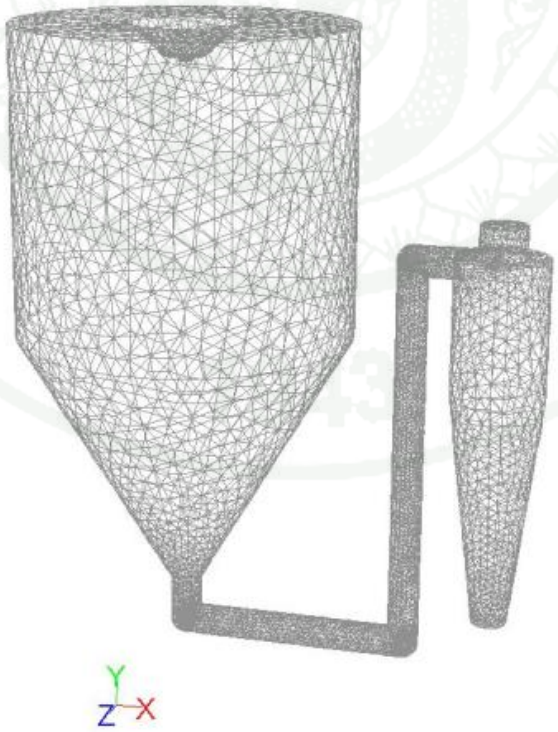

Figure 18 Mesh of the process spray dry (mm)

RESULTS AND DISCUSSION

The results of this research can be divided into five parts. The first part is the model to validate with the experiment data of Kieveit (1997) for the accuracy of the model. The second part is the model to predict the air flow pattern. The third part is the model to predict the particle residence time distribution. The forth part is the model to predict the occurrence of stickiness in the spray drying. The last part is create in spray drying process.

1. Validation of spray drying model

This section shows the results of three-dimensional CFD simulation in term of air velocity profile and air temperature profile in spray drying chamber. The results of prediction are validated by the experimental data of Kieveit (1997).

1.1 The air velocity profile

The CFD simulation of air velocity profile without spray in the spray dryer (Figure 19) shows that the flow field consists of a fast flowing downward core with a slow recirculation around that core near the upper section of the conical part of the chamber. The core broadens as going down to the outlet. The predicted and measured velocities at different levels of the spray chamber are depicted in Figure 20. For this case, the central core has the radius is about 0.2 m. The sharp descent of velocity magnitude at the axis of the chamber is reduced as the air moves down to the cone section of the chamber.The simulation results are shown in three grid resolutions (80,000 , 120,000 and 160,000 grids) and calculated the sum error value to compare all of them (shown in Appendix D). Simulation results show that 120,000 grids have sum error value in the acceptable criteria and spend the time to calculate in Fluent Program less than 160,000 grids. Therefore, this section shows the results of 120,000 grids.

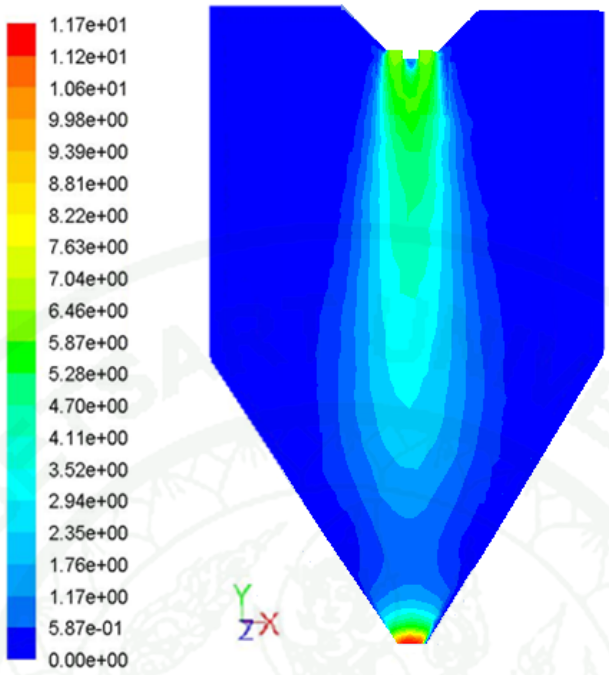

Figure 19 Contours of air velocity profile

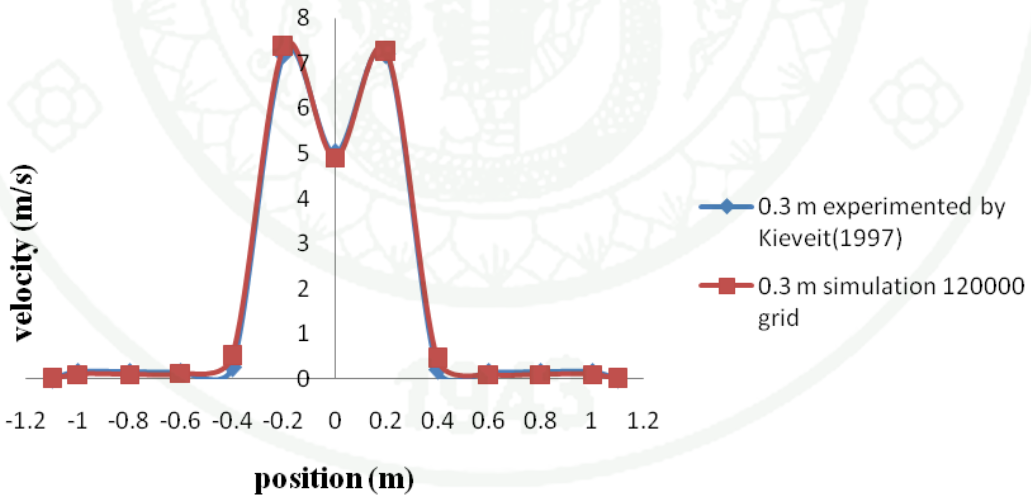

(a)

Figure 20 Comparison of air velocity profile at different levels of the spray chamber (a) 0.3 m, (b) 0.6 m, (c) 1.0 m. validation between simulation and experiment by Kieveit (1997)

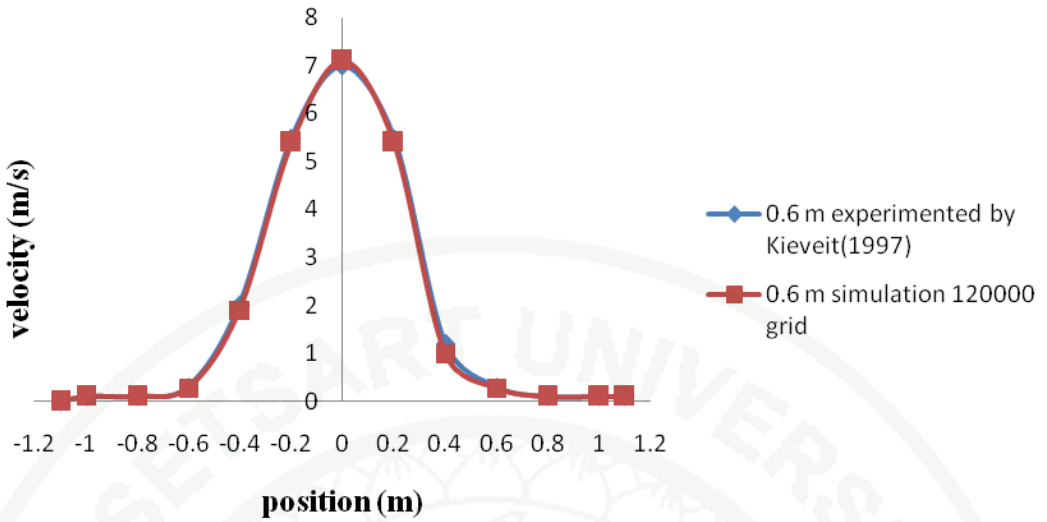

(b)

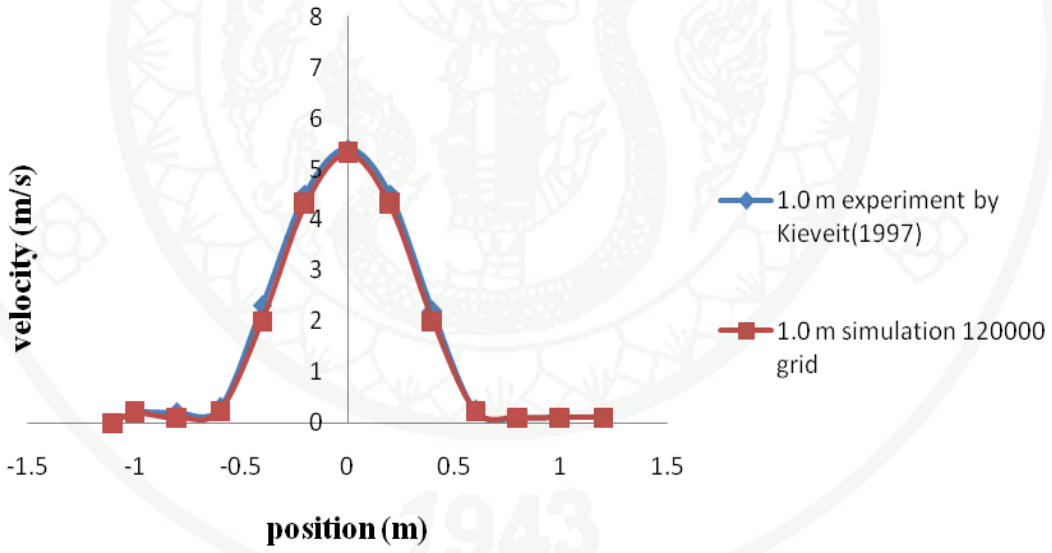

(c)

Figure 20 (Continued)

Figure 20 shows the comparison of the velocity profiles at different levels within the chamber between the simulation and Kieviet's experimental under no spray condition. Good agreement is obtained by considering the complexity of the process and measurement results. It is noted that there is a non-uniform velocity distribution in the core region of the chamber. The highest velocity magnitude is 7.36 m/s at the 0.30 m level from ceiling. The velocity is decreased as the air streams move downwards in the chamber. This trend is agreed very well with the experimental result. Only the prediction of velocity magnitudes at 1.0 m level is somewhat higher than the measured values. It is possibly due to the air flow revealing periodicity in the velocity magnitude at several locations in the chamber and the 1.0 m level is one of its. This nature of air flow was reported by Kieviet (1997) when measuring the velocity signal in these locations. Therefore, it implied that the air flow in the pilot plant spray dryer is naturally transient and the transient CFD modeling is required for this behaviour simulation.

1.2 The air temperature profile

The simulation of air temperature profile without spray in the spray dryer, is shown in Figure 21 under the pressure nozzle no spray conditions. The comparison between air temperature profile simulation and the experimental data by Kieviet (1997) at various levels are shown in Figure 22. It can be seen that the predicted results agree well with the experimental results.

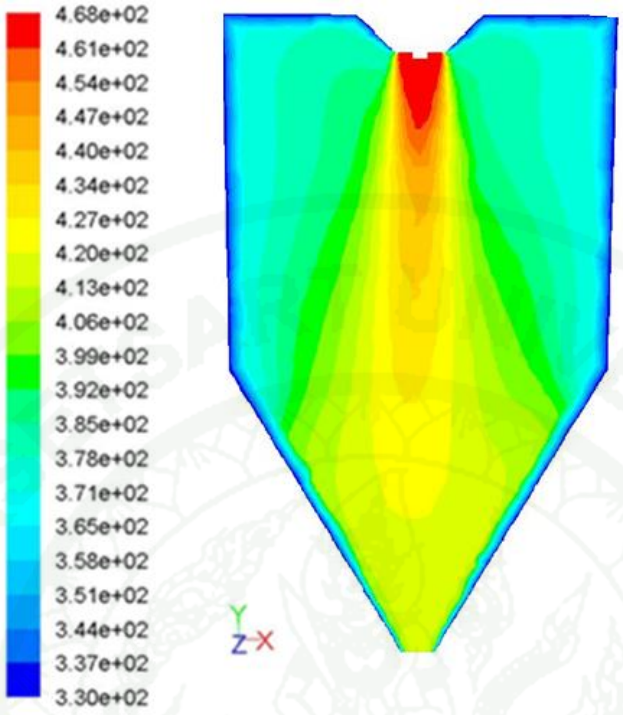

Figure 21 Contours of air temperature profile

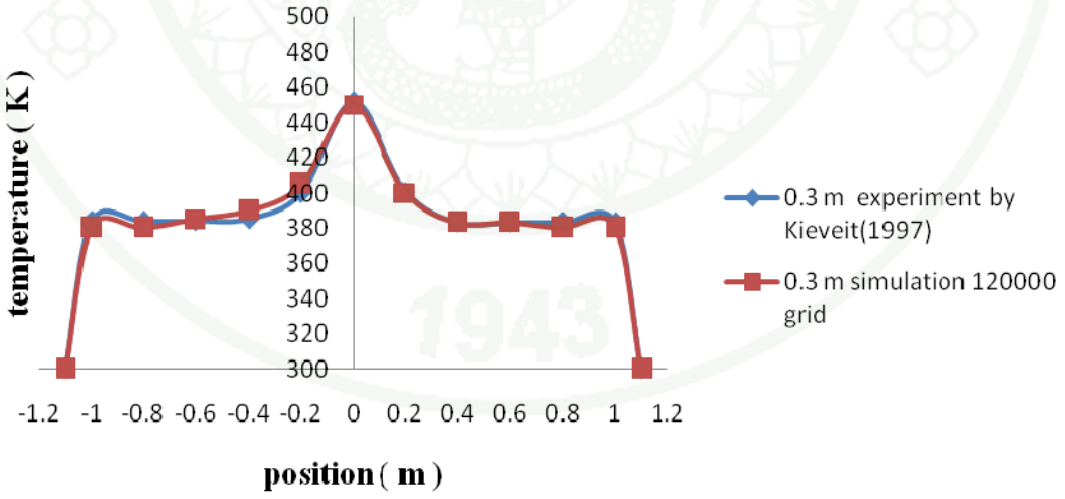

(a)

Figure 22 Comparison of air temperature profile at different levels of the spray chamber (a) 0.3 m, (b) 0.6 m, (c) 1.4 m. validation between simulation and experimented by Kieveit (1997)

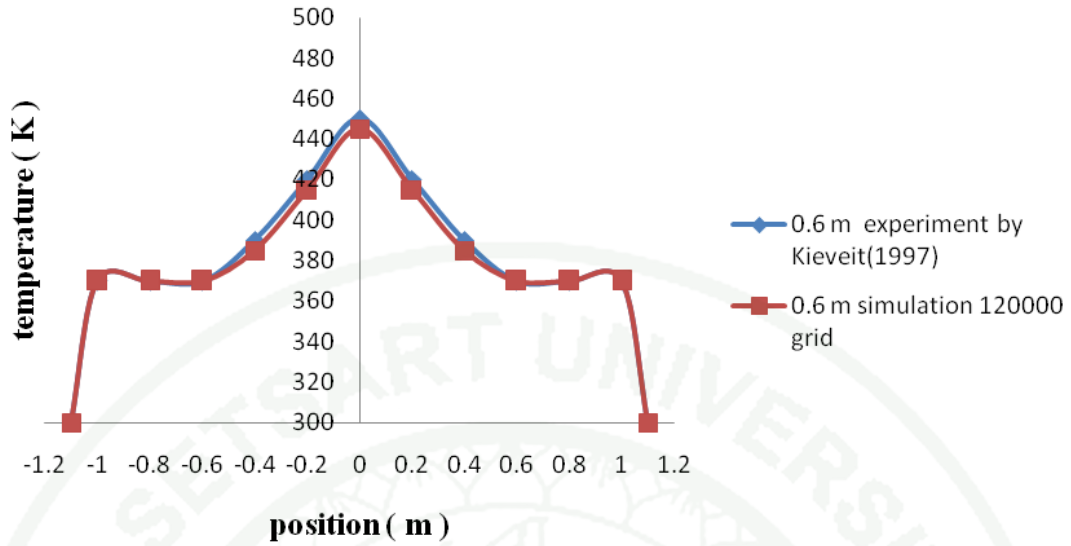

(b)

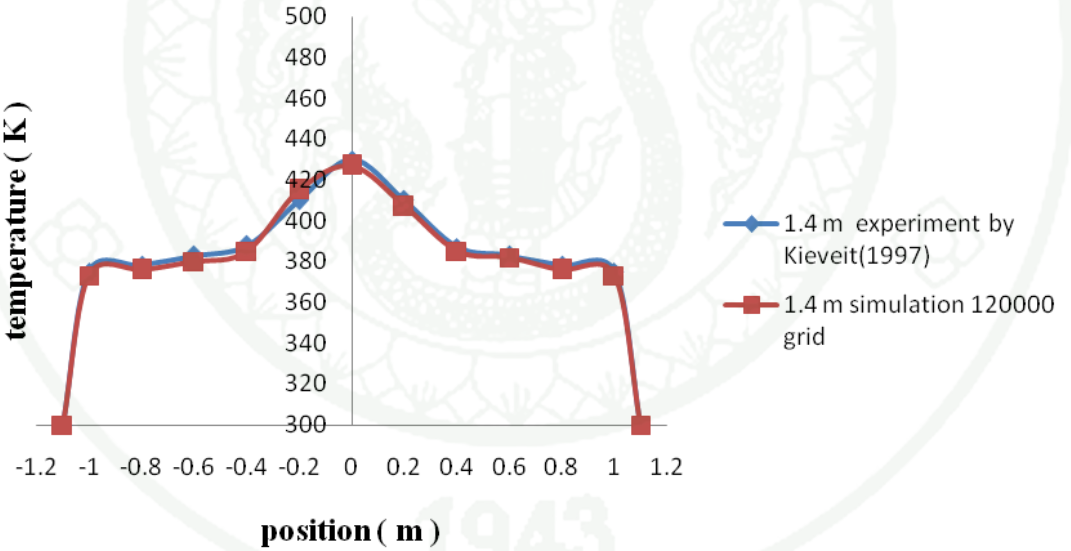

(c)

Figure 22 (Continued)

The air temperature profiles (Figure 21) show that the temperature in the central core region at a 2.2 m diameter is significantly different comparing with three at 0.3, 0.6, and 1.4 m levels. The prediction trend agrees very well with the trend of experimental results. The sharp descent of temperature at the axis of the chamber reduces as the air moves down to the cone section of the chamber. It can be seen that the predictions of temperature at 0.3, 0.6, 1.4 m levels are higher than the measured values. It is possibly due to the air flow revealing periodicity in the temperature at several locations in the chamber when measuring the temperature signal in these locations. Therefore, it can be said that the air flow in this pilot plant spray dryer is transient in nature and the transient CFD simulstion should be considered for this behavior simulation.

2. The vector plot of the air velocity

The velocity vector plot of air flow in the chamber is shown in Figures 23 and 24 the velocity vector plot and velocity streamline of air flow in the chamber. The air flow has only axial velocity component at the inlet. The flow field consists of a high velocity core flow zone and slow recirculation zone around the core. The core flow is extended toward the chamber outlet and the vortex flow is formed near the junction of the cylinder part and cone part. The vortex flow is extended up in the chamber around the core flow which is similar to the result presented by Kieviet (1997). The air flow pattern affects the particle flight paths and their drying rates. The main purpose of droplet/particle modeling as discrete phase is to simulate particle paths in the dryer, particle deposition on the wall and particle residence times.

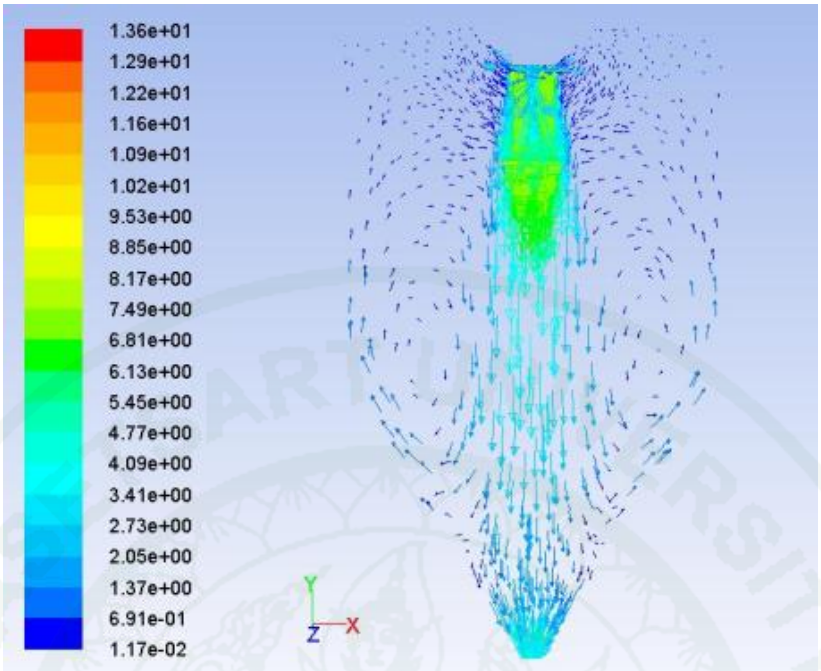

Figure 23 The vector plot of air velocity

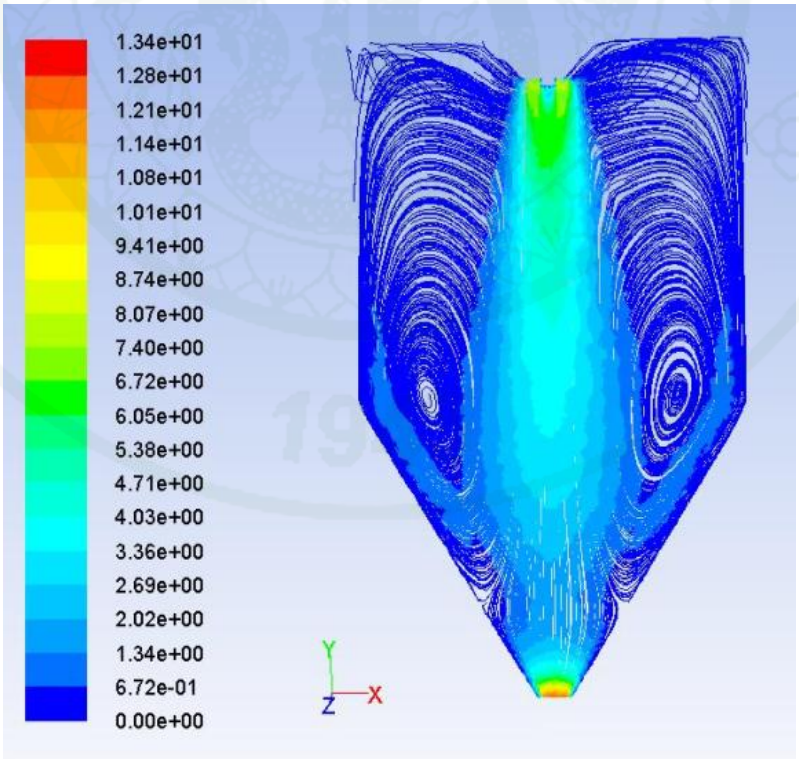

Figure 24 The streamline of air velocity

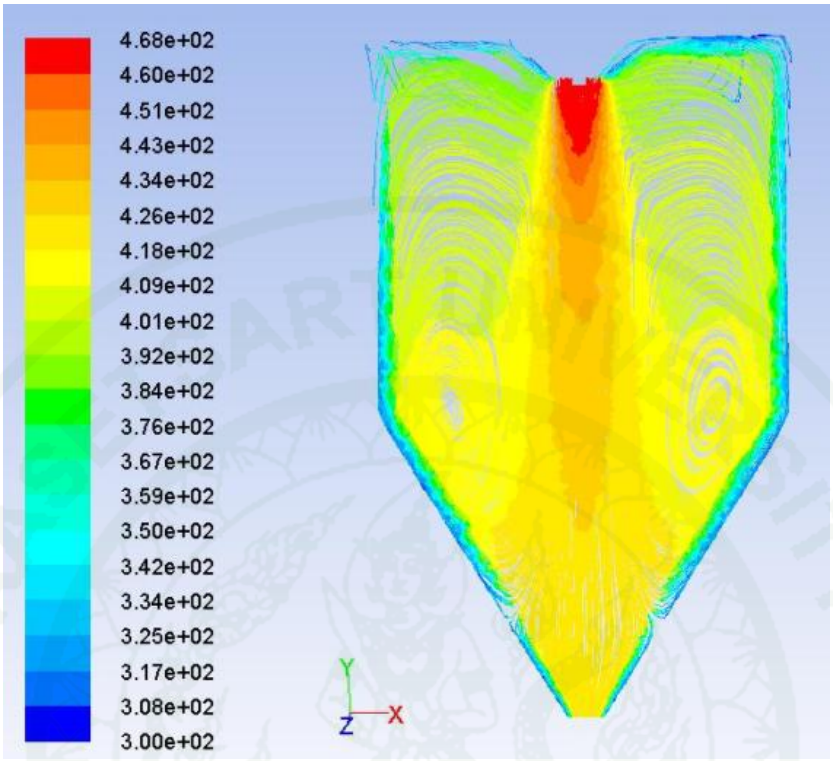

Figure 25 The streamline of air temperature

The streamline of air temperature flow in the chamber is shown in Figure 25. The system to the outside wall temperature is constant at 300 K and the wall is no heat transfer. The system considers air temperature flow in the chamber. It is found that the temperature will gradually transfer the heat from the high temperature to low temperature.

3. The particle residence time distributions

The particle residence time distributions of skim milk powder in the drying chamber. A parametric study carries out to investigate the effects of some important parameters: droplet diameter (40, 70, 100 μm) and inlet air temperature (433, 468 K) on the particle residence time in spray dryer. The pressure nozzle and the hollow cone spray pattern are used in this modeling. The droplets are sprayed continuously. The particle residence time in the chamber is determined from the time that the particles spend in the drying chamber since the particles leave from the nozzle until they exit the chamber. The mean residence time of predicted particles for various mean droplets diameter are shown in Table 3 and Table 4 and The predicted particles mean residence time for two levels of inlet air temperatures are shown in Table 5 and Table 6 .

Table 3 The particles mean residence time of mean droplets diameter

Mean droplet diameter (μm)	Mean Residence time (s)
40	1.6
70	1.4
100	1.6

Table 3 presents the effect of mean droplet diameter on particles mean residence time. The mean residence time of droplet diameter is estimated for 3 runs. The results show that the mean droplet diameter has significant effect on the particle residence time. The model bases on the air flow pattern behavior inside the spray dryer and gravity effect. An increase in droplet size causes a decrease in residence time because the small droplet does not have enough momentum to escape from the core flow; therefore they followed the air flow pattern. The large droplet falls down by the force of gravity, therefore the larger particles have smaller residence time than the larger particle (the mean residence time of 40, 70 and 100 μm is 1.6, 1.4 and 1.2 second, respectively) which is similar to the result presented by Omid *et al*. (2009).

Table 4 The particle residence time in the spray drying chamber

Mean droplet size (μm) / Residence time (s)	40 μm	70 μm	100 μm
0.2	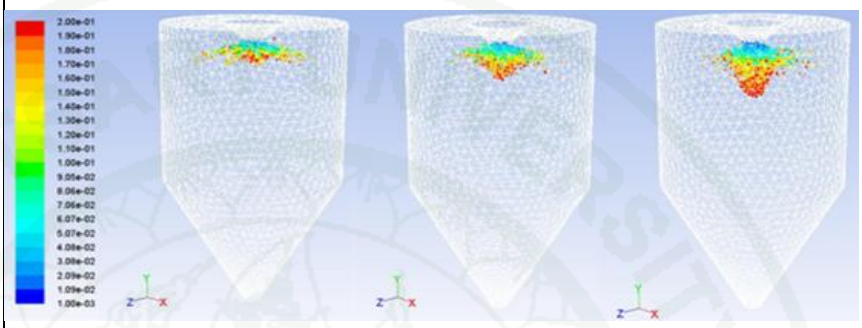		
0.4	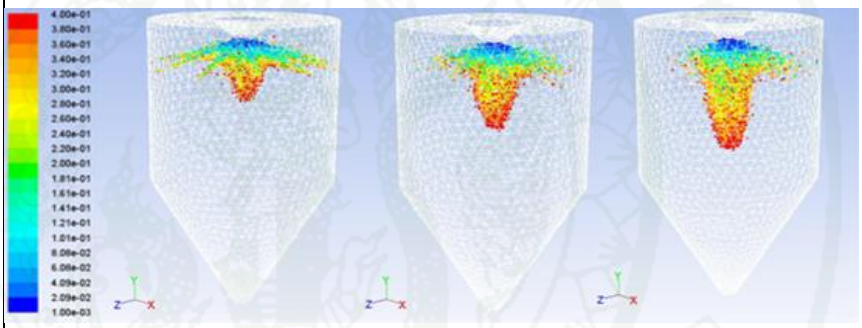		
0.6	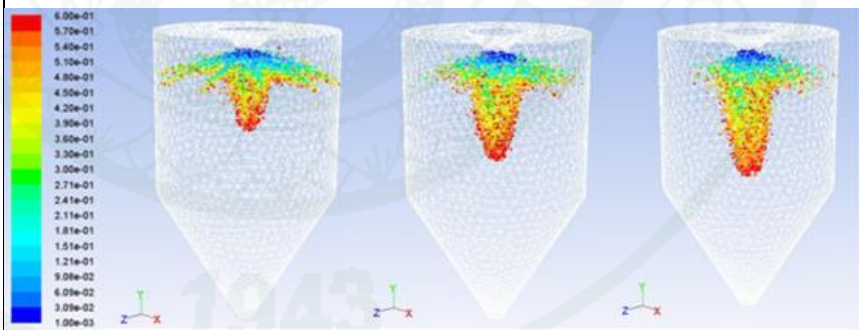		
0.8	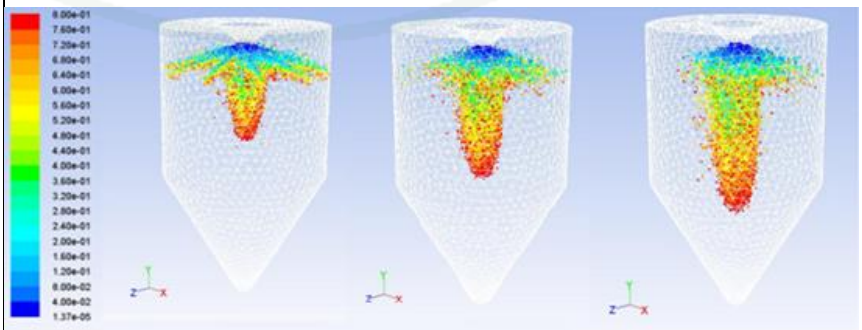		

Table 4 (continued)

Mean droplet size (μm) / Residence time (s)	40 μm	70 μm	100 μm
1.0	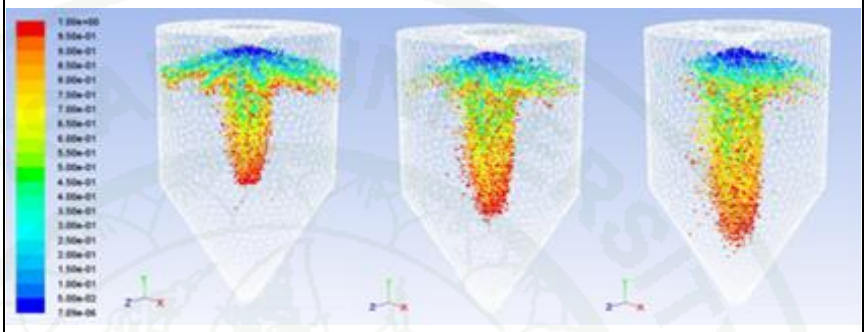		
1.2	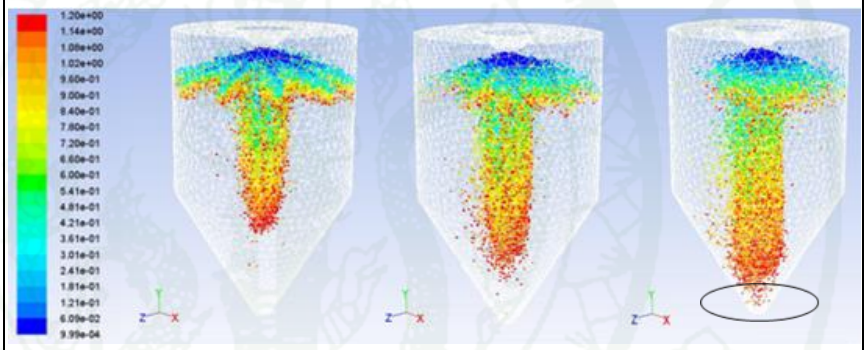		
1.4	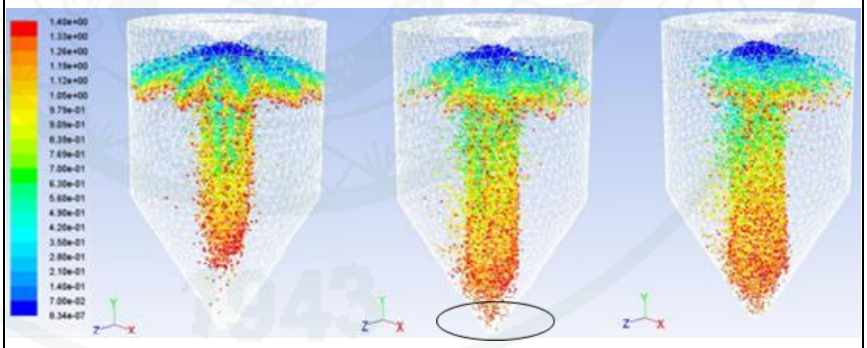		
1.6	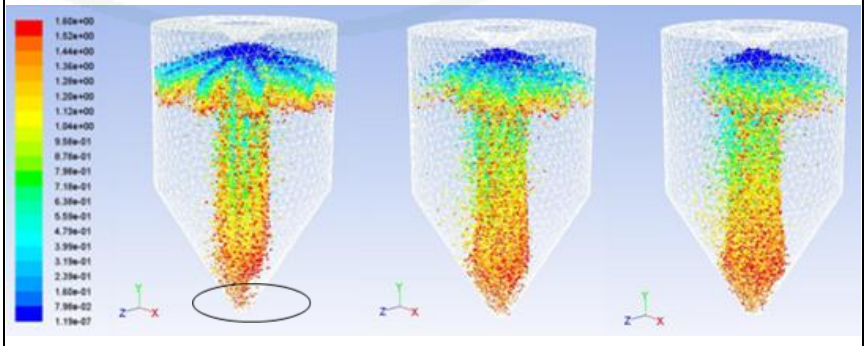		

In this system, the inlet air velocity and the injection velocity are fixed as constant, and the particle sizes 40 μm, 70 μm, and 100 μm are tested to observe the effect of particle size on the stickiness of milk and residence time in drying chamber. Table 4 shows the particle residence time in the dry chamber. The red region represents the particle which stays for long time in the dry chamber, and the blue region is the particle which is introduced into the dry chamber. Table 4 shows the distribution of particle at 0.2 seconds. The large particle will be ready to settle than the small particle due to the gravity.

Table 5 The particles mean residence time in two levels of inlet air temperatures

Temperature (K)	Mean Residence time (s)
433	1.38
468	1.39

Table 5 presents the effect of the air inlet temperature on particle mean residence times. The results show the simulation in case of the mean droplet diameter of 70 μm. From the results shown in Table 6, the mean residence time of 433 K and 468 K are 1.38 and 1.39 seconds, respectively. It can be found that the results showed no significant difference between the mean residence times of particles for both levels of inlet air temperatures. In this system, the inlet air velocity and the injection velocity are fixed as constant, and the particle sizes 70 μm is tested to observe The particle mean residence time in two levels of inlet air temperatures in Table 6. The red region represents the particle which stays for long time in the dry chamber, and the blue region is the particle which is introduced into the dry chamber. Table 6 shows the distribution of particle at 0.2 s – 1.39 seconds.

Table 6 The particles mean residence time in two levels of inlet temperatures

Inlet temperature (K) / Residence time (s)	433	468
0.2	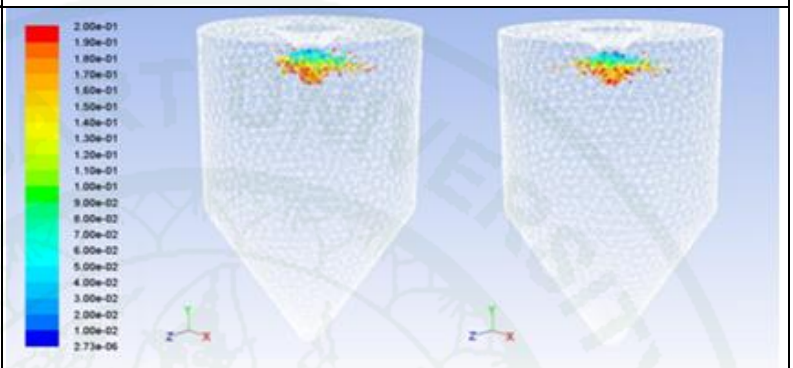	
0.4	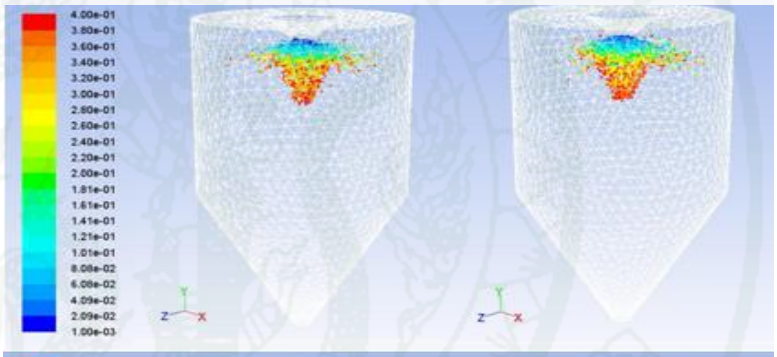	
0.6	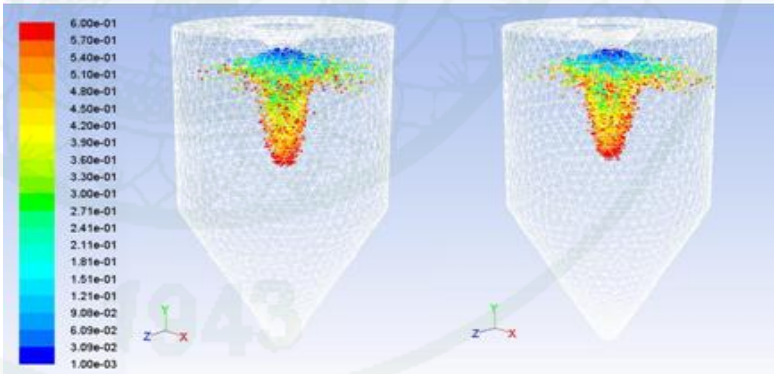	
0.8	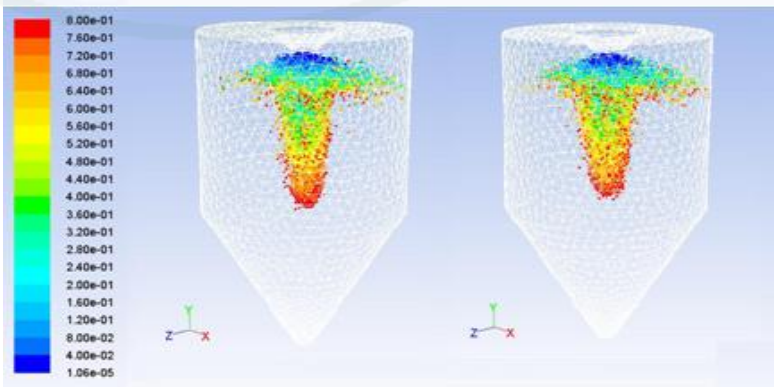	

Table 4 (continued)

Residence time (s) \ Inlet temperature (K)	433	468
1.0	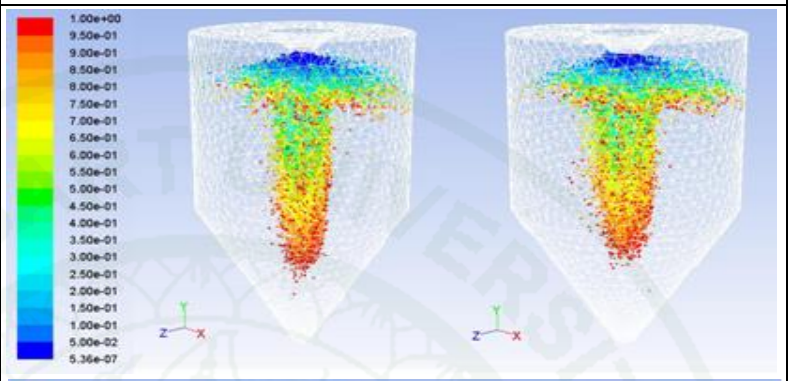	
1.2	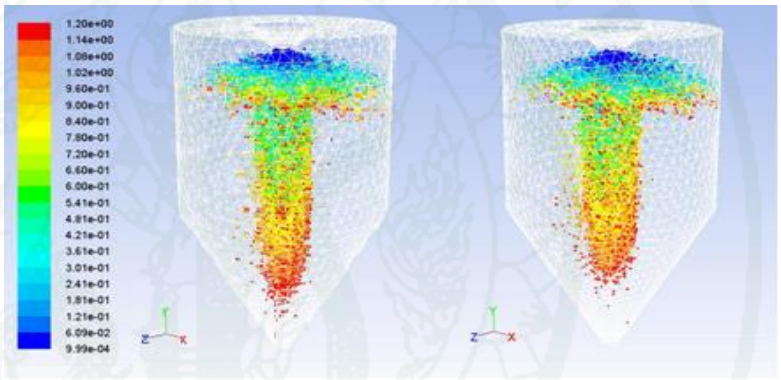	
1.38	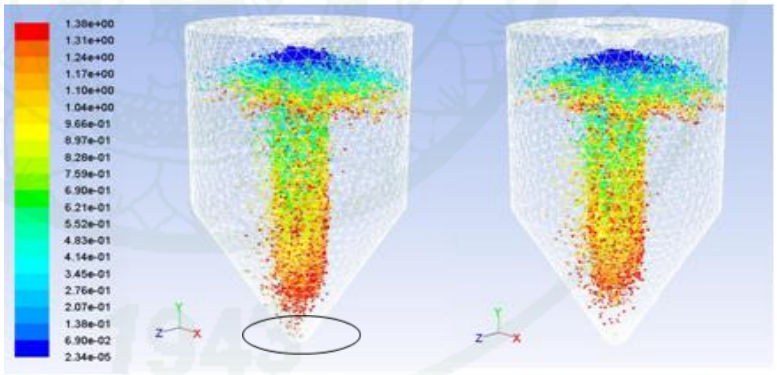	
1.39	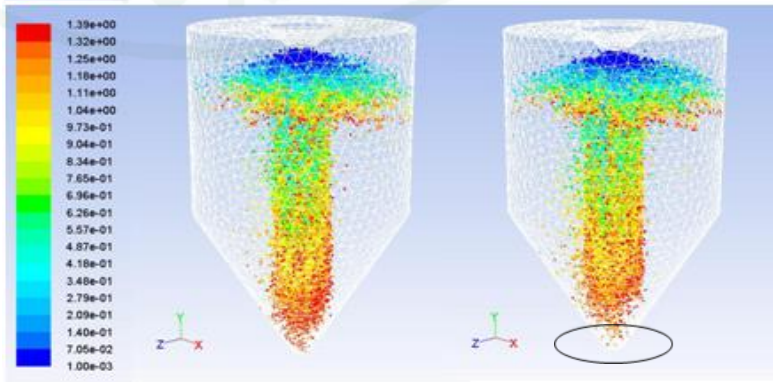	

4. The stickiness of spray drying model

The spray drying simulation for skim milk powder using computational fluid dynamic to predict the stickiness. The stickiness is the phenomena that commonly encounters during spray drying process. In this work, we do vary droplet of size 40, 70 and 100 microns. The incident of stickiness depends on the main factors: a temperature and air humidity in the droplet. Fluent Program considers fluid mainly, therefore result shows as Figures 26 and 27. From the equation of heat and mass transfer, the droplet 40 micron has surface area of heat and mass transfer more than 70 and 100 microns, the result conforms to the theory Master (1987) that is the droplet 40 micron from a temperature profile then it shows that the heat transfer is better than 70 and 100 microns and it conforms to the profile of humidity that is the droplet 40 micron, it has a good mass transfer like the picture that the small droplet has high air humidity in a chamber, so if we consider the droplet. The large particle has the higher humidity in droplet than the small one.

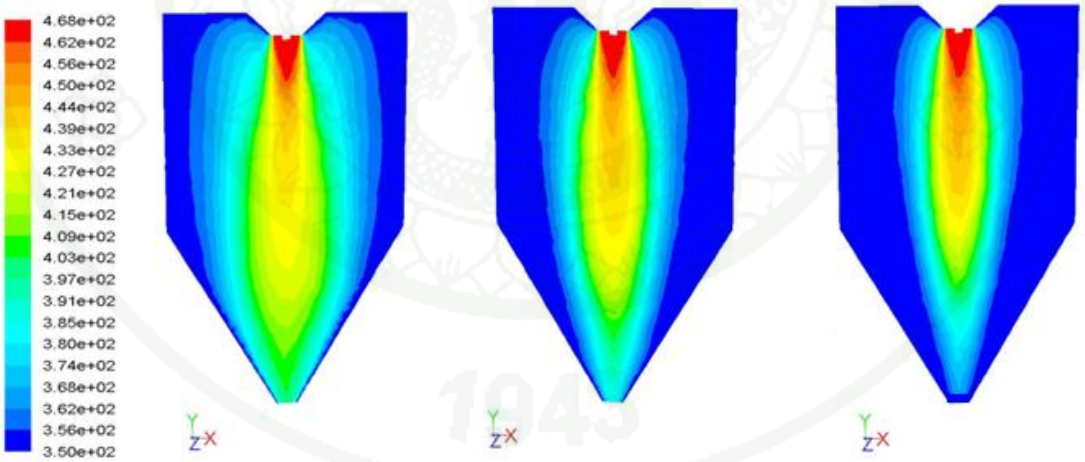

Figure 26 The temperature of chamber in spray drying model

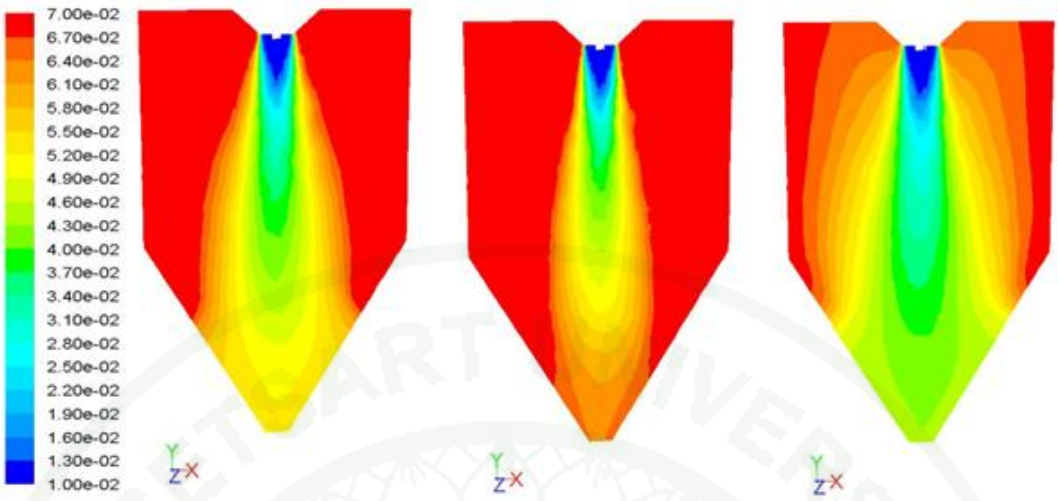

40 μm 70 μm 100 μm

Figure 27 The moisture content of chamber in spray drying model

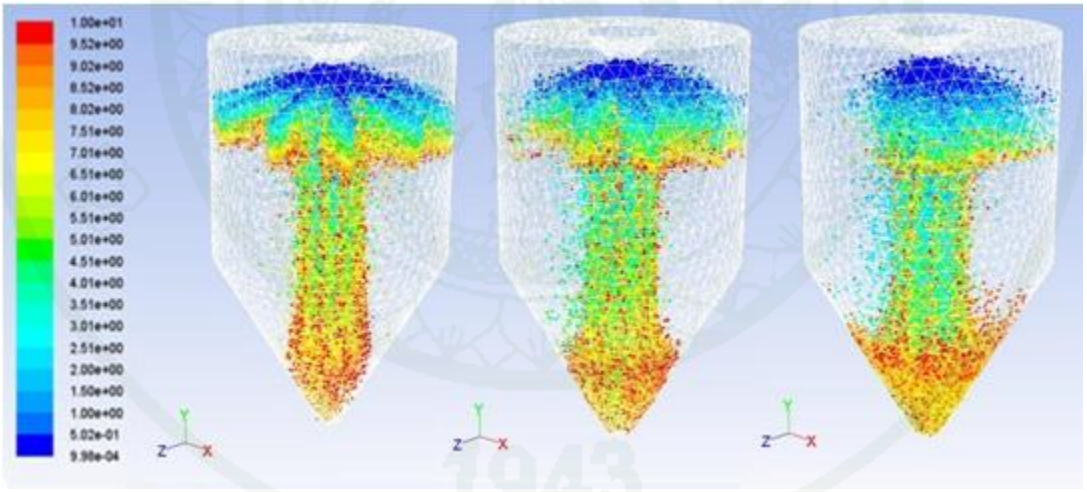

40 μm 70 μm 100 μm

Figure 28 The stickiness of chamber in spray drying model

Figure 28 shows the particle residence time in the spray drying chamber at spray injections of 10 second are 40, 70 and 100 μm, respectively. The red region represents the particle which stays for long time in the dry chamber, and the blue region is the particle which is introduced into the dry chamber. A bigger particle (100 μm) can penetrate the fast flowing core into the slow recirculation zone whereas the smaller particles. Stickiness deposition mainly occurs on the conical wall and the least deposition occurs on the cylindrical wall of the chamber The increment of the mean droplet size causes an increase in the stickiness rate because the large particle has the higher humidity in droplet than the small one.

5. The plant design spray drying process

The spray drying simulation for skim milk powder using computational fluid dynamic is to the created plant in spray drying process. This section describes separation of particles from a flow with high velocity, we add a cyclone. Figure 29 shown spray drying process. The picture is that the entrance of air is high and gradually decreases until the exit velocity of the air chamber is very high up. Then the air will flow through the pipe to the cyclone, which shows that the elbow is a very high speed due to the angular velocity and principles that we use to separate particles from the air. We will use this center for the centrifugal principle. Large particles will fall with the force of gravity of the lighter air will fly out over the top of the cyclone.

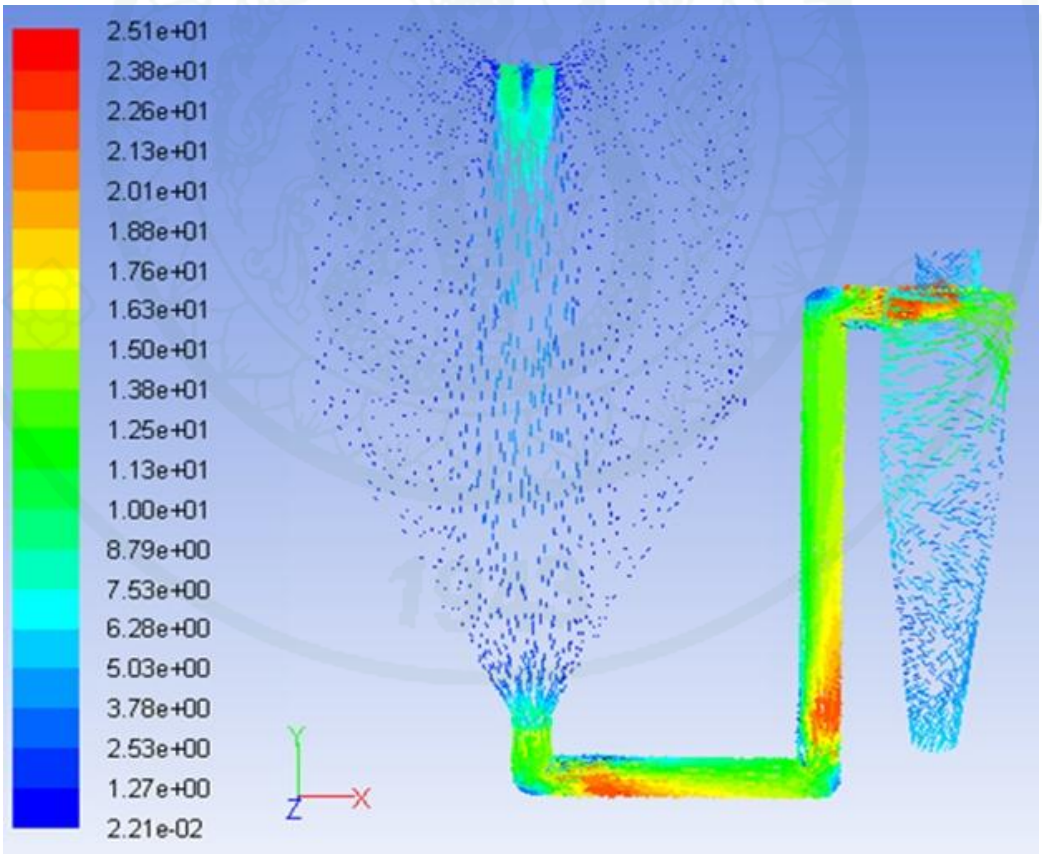

Figure 29 The process of spray drying

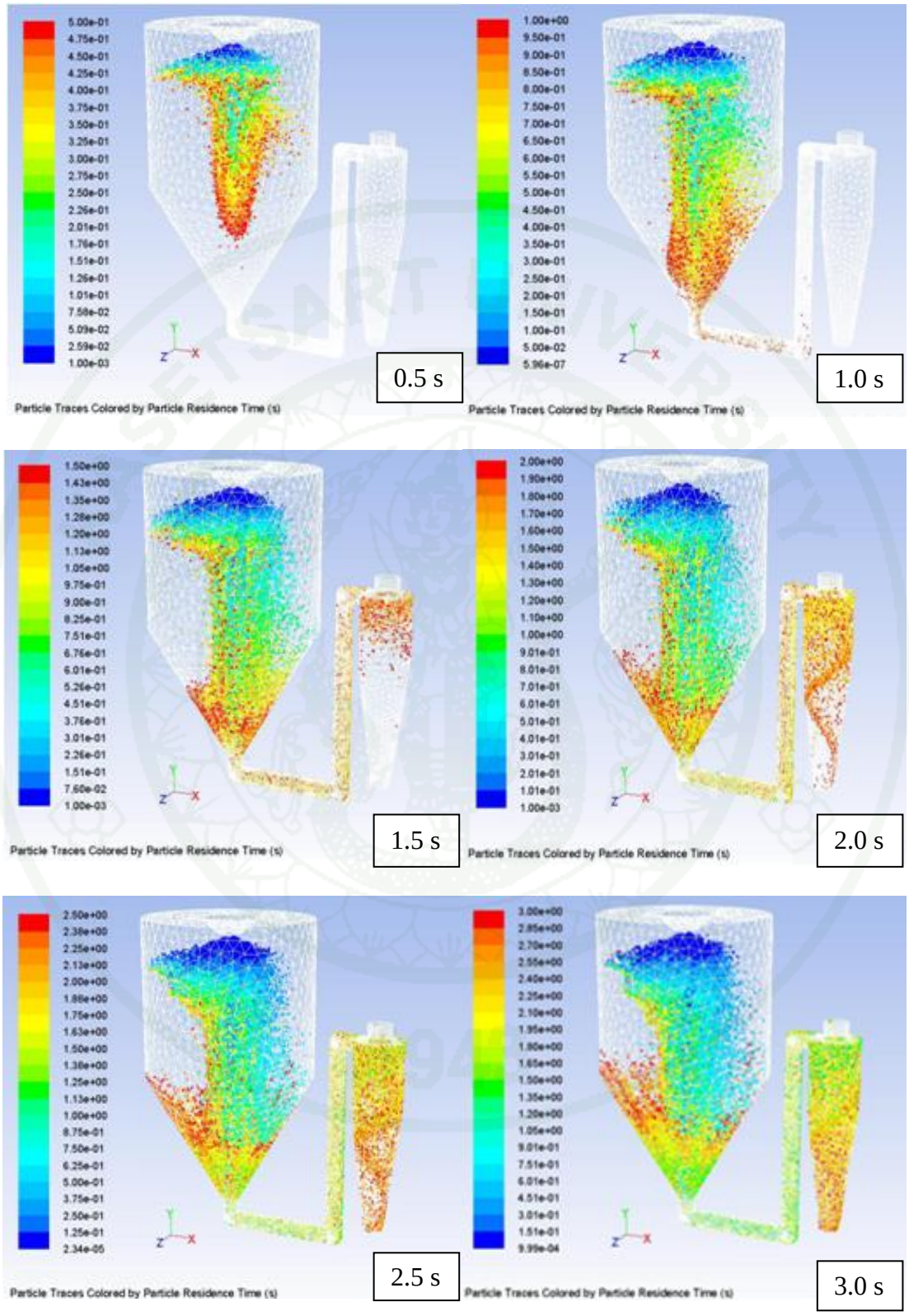

Figure 30 The residence time of spray drying process

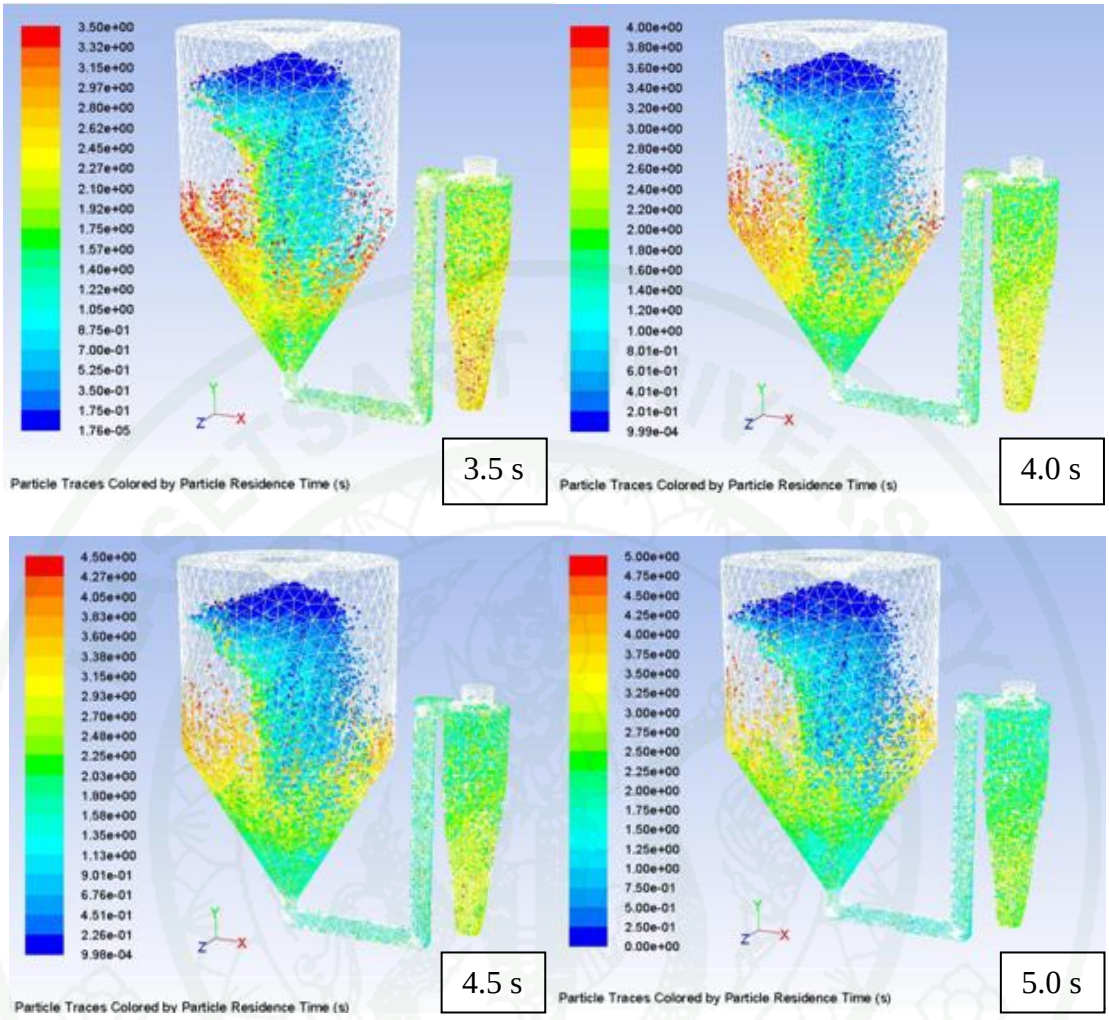

Figure 30 (continued)

The Figure 30 shown the residence time of spray drying process at 0.5 to 5 seconds found that the particles will begin to dry out the room for 3 second, we will be able to separate particles from the air flow speed. This is consistent to the result of Master (1987).

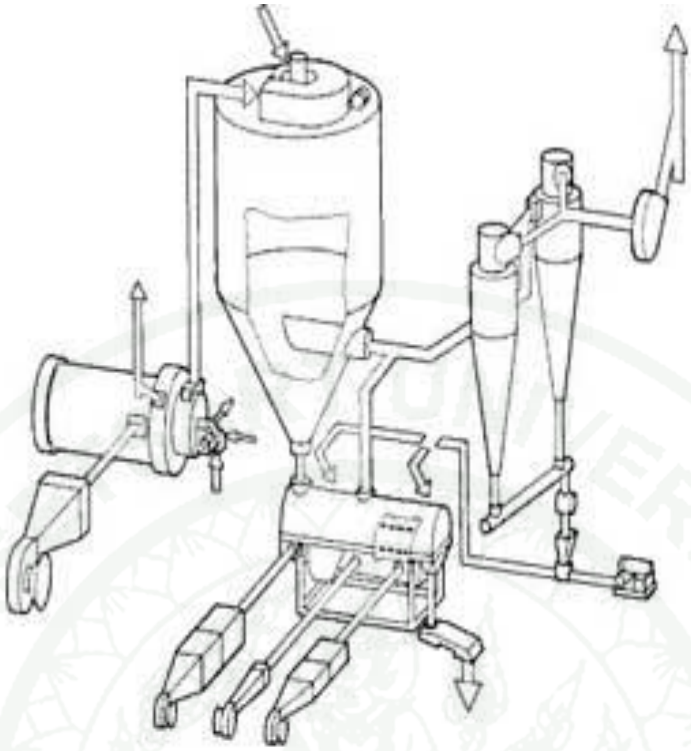

Figure 31 The process of spray drying in industry

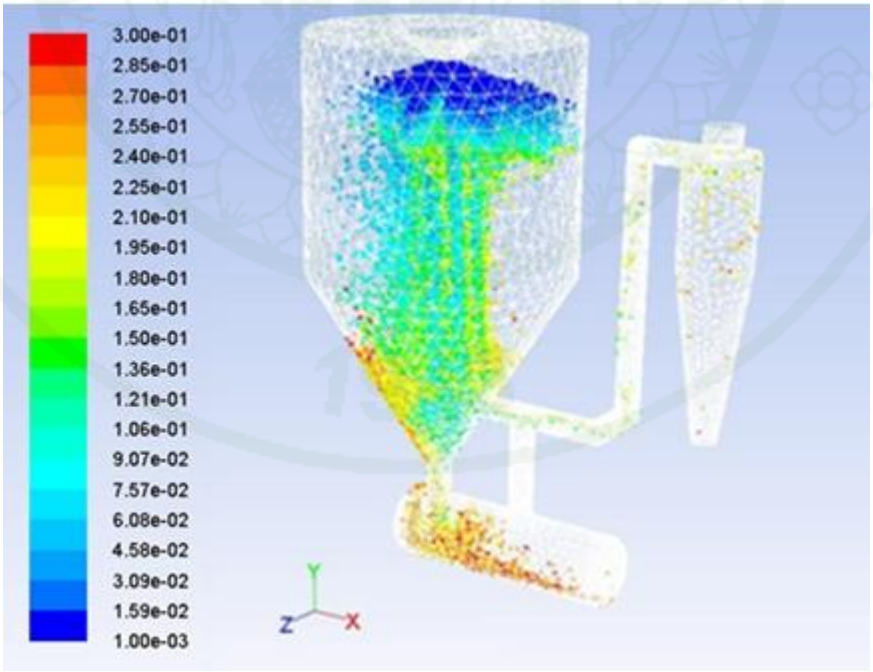

Figure 32 The residence time of spray drying process in industry

This part describes the system of spray dryer simulation which is designed to be similar to the real industry system as shown in Figures 31 and 32. This figure shows that there is an outlet pipe connected from spray dryer to a cyclone. Most of sprayed particles fall into the bottom due to the gravity. The light particle can escape from the spray dryer to cyclone. The function of spray dryer is to trap the light particle which escapes from the spray dryer. In cyclone, the feed is introduced in the tangential velocity, and then its centrifugal force due to swirling effect throws the large material against the wall. The large particle will be draged into the underflow of the cyclone. Figure 32 shows transient simulation result of the spray dryer at t =3 s. The possibility of milk production loss in the real system might occur in cyclone due to the stickiness of milk. When the milk particle is thrown against the wall, sticky milk can deposit on the cyclone wall. If a lot of milk scale on the wall, the process must be shut down for the maintenance.

CONCLUSION AND RECOMMENDATION

Conclusion

The stickiness is phenomena that happened during the spray drying process. These phenomena are important since they can be a beneficial process using for controlling the enlargement of particles to improve powder properties and obtain high-quality products. However, it can be a cause of some problems during spray drying process which is a cyclone blockage. This makes these phenomena is particularity interesting to study.

In this work, the spray drying model was simulation air flow, temperature profile and residence time distibution for skim milk powder in spray dryer. In addition, the stickiness of skim milk powder also was investigated. The spray drying model was divided into five major parts. The first part was the model to validate with the experiment data of Kieveit (1997) for the accuracy of the model. The second part was the model to predict the air flow pattern. The third part was the model to predict the particle residence time distribution. The forth part was the model to predict the occurrence of stickiness in the spray drying. The last part was created in spray drying process.

The three-dimensional computational fluid dynamic (CFD) simulation in a co-current pilot plant spray dryer fitted with a pressure nozzle for spray dryer skim milk powder. Good agreement was obtained in the published experiment data where the CFD simulations correctly predict the internal behavior of the spray dryer. It discerned that the air flow at specified conditions consist of fast flowing core and slow recirculation zone around it. The drying of droplet takes place in the core region where the smaller droplets evaporated due to high air temperature. The air flow pattern have an important effection upon the trajectories of the particles, therefore the smaller particles have the longer residence time than the larger particle (the mean residence time of 40, 70 and 100 μm were 1.6, 1.4 and 1.2 second respectively.)

Stickiness deposition mainly occurred on the conical wall and the least stickiness deposition occurred on the cylindrical wall of the chamber. Increasing the droplet size caused an increase in fraction of stickiness deposition on the wall.

Recommendation

1. The model should be validated with the experimental data for the accuracy of the model.
2. The stickiness process of powder may be studied using Computational Fluid Dynamics (CFD) program combine with Distinct Element Method technique.
3. Heat transfer between particle-particle and particle-wall may take into account to make the results more correct.
4. The stickiness process of powder may be studied using Computational Fluid Dynamics (CFD) code combine user define function (UDF).

LITERATURE CITED

Anderson, J.D. 1984. **Computational fluid dynamics-The basics with applications**. McGraw-Hill Inc. New York.

Bakker, A. 2002. **Computational fluid mixing**.. Fluent Inc., Lebanon USA

Cham Processes dairy. 2006. **Milk Powder**. Available Source: http://nzic.org.nz/ChemProcesses/dairy/3C.pdf,May 26, 2010.

Chen, X. D., M. M. Farid., D. Reid., A. Fletcher.,and D. Pearce., 1999. A new model for the drying of milk droplets for fast computation purposes. **CHEMECA99**. Newcastle. Australia.

Fluent Manual. 2010. Discrete phase models. Available Source: http://www.fluent.com,April 28, 2010.

Gordon, M. and J.S. Taylor. 1952. Ideal copolymers and the second-order transitions of synthetic rubbers. I Non-crystalline copolymers. **International Journal of Applied Chemistry**. (2):493-500.

Huang, L., K. Kumar and A.S. Mujumdar. 2003. A parametric study of the gas flow patterns and drying performance of co-current spray dryer: Result of a computational fluid dynamics study. **Drying Technology**. 21(6):957-978.

Kieviet, F.G., 1997a. **Modeling quality in spray drying**. Ph.D. thesis. Endinhoven University of Technology. The Netherland.

———, R. Van and P.J.A.M. Kerkhof. 1997b. Measurement and modeling of the air flow pattern in a pilot-plant spray dryer. **Chemical Engineering Research and Design**. (75):321-328.

Kieviet, F.G, P.J.A.M. Kerkhof. 1997c. Air flow, temperature and humidity patterns in a co-current spray dryer: Modelling and measurements. **Drying Technology**. 15(6):1763-1773.

Lefebvre, A.H., 1989. **Atomization and Sprays**, Hemisphere Publishing Corporation, United States of America. (2):173-180.

Masters, K., 1985.**Spray Drying Handbook**, Fifth edition. John Wiley and Sons. New York.

McCabe, W.L., J.C. Smith and P. Harriott. 1993. **Unit Operations of Chemical Engineering**. McGraw-Hill, New York. (5):824-826.

McCarthy, O.J. and H. Singh. 2004. Physico-chemical Properties of Milk. **Advanced Dairy Chemistry**. Massey University, Palmerston North, New Zealand.

Mezhericher, M., A. Levy and I. Borde. 2010a. Modeling of droplet drying in spray chambers using 2D and 3D computational fluid dynamics. **Drying Technology**. (19):257-268.

——— , ——— and ———. 2010b. Droplet-droplet interactions in spray drying using 2D computational fluid dynamics. **Drying Technology**. (26):265-282.

——— , ——— and ——— . 2010c. Spray drying modeling based on advanced droplet drying kinetics. **Chemical Engineering and Processing**. (49):1205-1213.

Omid, R.R and M. Hosseinalipour. A proposed numerical-experimental method for drying kinetics in a spray dryer. **Journal of Food Engineering**. (90):20-26.

Ozmen, L. and T.A.G. Langrish. 2002. Comparison of glass transition temperature and sticky point temperature for skim milk powder. **Drying Technology**. (20):1177-1192.

Pietsch, W., 2003. An interdisciplinary approach to size enlargement by agglomeration. **Powder Technology**. (130):8-13.

Process Spray Drying. 2005. **Spray Drying**. Available Source: http://www.malvern.com/ProcessEng/images/processes/spray_drying_overview1.gif, August 17, 2009.

Rinil, K and C. Anandnaramakrishnan. Computational fluid dynamics (CFD) applications in spray drying of food product. **Food Science & Technology**. (21):383-398.

Roos, Y.H., 2002. Importance of glass transition and water activity to spray drying and stability of daily powders. **EDP Sciences Journal**. (10):475-484.

Saad, N.S., 2010. CFD Simulation of a co-current spray dryer. **Engineering and Technology Journal**. (62):25-34.

Versteeg, H.K. and W. Malalasekera. 1995. An Introduction to Computational Fluid Dynamics The Finite Volume Method. **Longman Scientific & Technical**. (7):1-35.

Williams, A.M., J.R. Jones, A.H.J. Paterson and D.L. Pearce. 2009. Effect of fines on agglomeration in spray dryers: An experimental study. **International Journal of Food Engineering**. (5):1-8.

Warsi, Z.U.A., 1992. **Fluid Dynamics Theoretical and Computational Approaches,** CRC press, Florida. (8):1-56.

APPENDICES

Appendix A

Boundary conditions used for simulation

Appendix Table A1 Boundary conditions used for simulation

Property	Value
Air mass flow rate (kg/s)	0.336
Air temperature (□K)	468
Air velocity (m/s)	7.36
Spray flow rate (kg/s)	0.0139
Spray cone angle	76
Velocity at the nozzle (m/s)	59
Feed temperature (□K)	300
Turbulence *k* - value (m^2/s^2)	0.027
Turbulence ε - value (m^3/m^2)	0.37
Pressure at outlet (Pa)	-100
Chamber wall thickness (m)	0.002
Wall material	Steel
Wall-heat transfer coefficient (W/m^2K)	3.5
Interaction B.C. between wall and droplet	Refect
The spray of droplets is assumed to have solid	42.5 %

Appendix B

Property of skim milk powder

Appendix Table B1 Property of skim milk powder

Property	Value
Density (kg/m^3)	1,549
C_p Specific heat (j/kg-K)	1,790
Thermal Conductivity (W/m-K)	0.03356
Viscosity (poise)	0.0179
Latent Heat (j/kg)	2,277,000
Boiling point (K)	373
Mass diffusivity (m^2/s) Chen et al, 1999	270,000
Saturation Vapor pressure (pascal)	93,289
Droplet surface tension (N/m) O.J. McCarthy, 2002	0.04729

Appendix C

Droplet Collision Model

Droplet Collision Model

The probabilistic model developed by O'Rourke is used to address the effect of droplet–droplet collisions.O'Rourke's algorithm is based on the concept of parcels of droplets, where each parcel represents a group of droplets with the same properties When two parcels are present in the same continuous-phase cell, they are likely to collide. In this case, the parcel of droplets with the larger diameter is designated the ''collector'' (contains n1 droplets) and the parcel of droplets with the smaller diameter is designated the ''contributor'' (contains n2 droplets). A mean expected number of collisions that the collector undergoes is given by

$$\bar{n} = \frac{n_2 \pi (r_1 + r_2)^2 u_r \Delta t}{V} \tag{C.1}$$

where r_1 and r_2 are radii of the collector and contributor droplets, u_r is the relative velocity, Δt is calculation time step, and V is the cell volume. According to O'Rourke, the probability distribution of the number of collisions experienced by collector, m follows a Poisson distribution

$$P(m) = e^{-\bar{n}} \frac{\bar{n}^m}{m!} \tag{C.2}$$

The probability of at least one collision between the two droplets under consideration, $P_1 = 1 - P(m \geq 1)$ is complementary to the probability of no collisions, $P(m = 0)$

$$P_1 = 1 - P(m = 0) = 1 - e^{-\bar{n}} \tag{C.3}$$

We consider the interaction between two parcels when the probability of at least one collision exceeds a critical value $P_1 \geq 0.5$. In that case, using Eq. (3) we can evaluate a critical value of the mean expected number of collisions

$$\bar{n}_{cr} = -\ln 0.5 = 0.69315 \tag{C.4}$$

Correspondingly, the collisions between the droplets of two parcels are assumed to occur when $\bar{n} \geq \bar{n}_{cr}$.

The critical offset is calculated by O'Rourke using the expression

$$b_{crit} = (r_1 + r_2)\sqrt{\min\left(1.0, \frac{2.4f}{We}\right)} \tag{C.5}$$

Where f is a function of r_1/r_2 defined as

$$f\left(\frac{r_1}{r_2}\right) = \left(\frac{r_1}{r_2}\right)^3 - 2.4\left(\frac{r_1}{r_2}\right)^2 + 2.7\left(\frac{r_1}{r_2}\right) \tag{C.6}$$

$$We_c = \frac{\rho u_r^2 (r_1 + r_2)}{\sigma} \tag{C.7}$$

The value of the actual offset between two droplet centers is estimated by:

$$b = (r_1 + r_2)\sqrt{R_m} \tag{C.8}$$

where R_m is a random number 0 and 1. By comparing b and b_{cr} the type of collision can be established.Thus, if $b < b_{cr}$ the result of the parcel's collision is coalescence, in which each droplet of the collector coalesces with a contributor droplet to form an agglomerate on a one-to-one basis. If there is an excess of droplets in the contributor, they remain in the contributor, to be tracked in the next computational step. The velocities of the agglomerate and of remaining droplets within the contributor are determined by the law of conservation of momentum, and the corresponding contact forces are found using Newton's second law. The radius of the collector increases after coalescence according to volume conservation:

$$r_{1,new}^3 = r_1^3 + r_2^3 \quad \text{(C.9)}$$

Appendix D

Result test sum error number grid

Appendix Table D1 Sum error of air velocity profile at different levels of spray chamber

Number of grid / Distance(m)	80,000	120,000	160,000
0.3	9.6 %	4.2 %	3.1 %
0.6	10.2 %	4.4 %	2.7 %
1.0	11.1 %	4.7 %	3.3 %

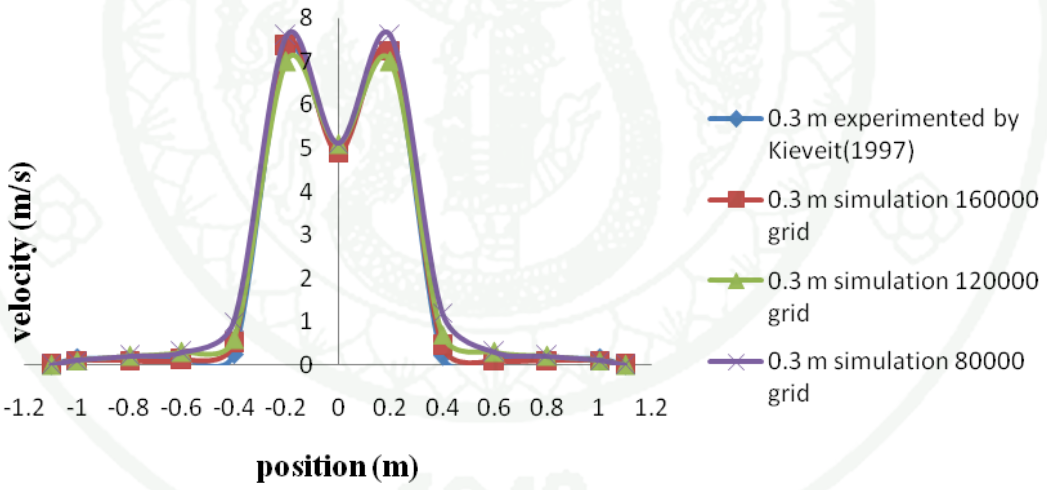

(a)

Appendix Figure D1 Comparison of air velocity profile at different levels of the spray chamber (a) 0.3 m, (b) 0.6 m, (c) 1.0 m. validation between simulation and experiment by Kieveit (1997) very number of grid at 80,000 , 120,000 and 160,000

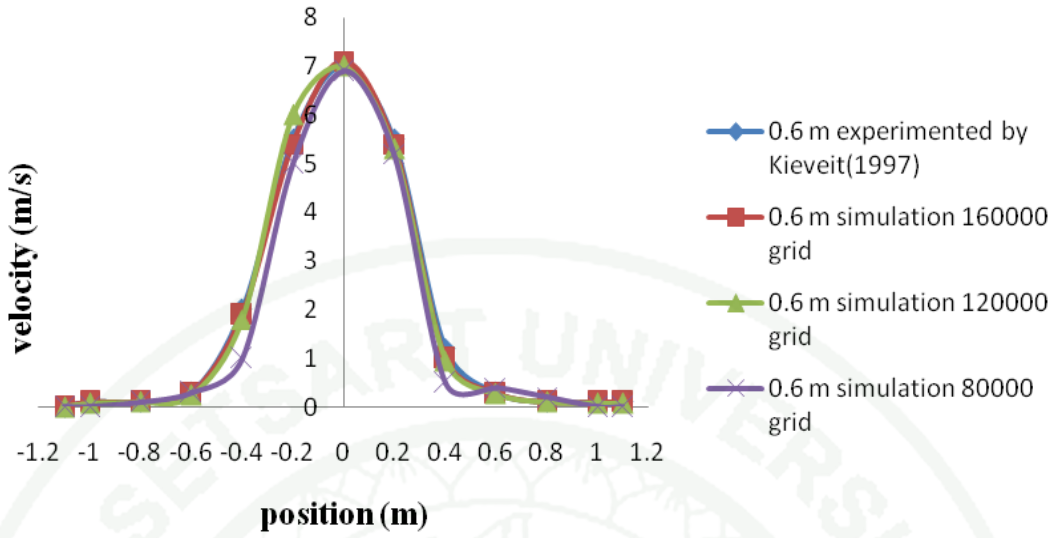

(b)

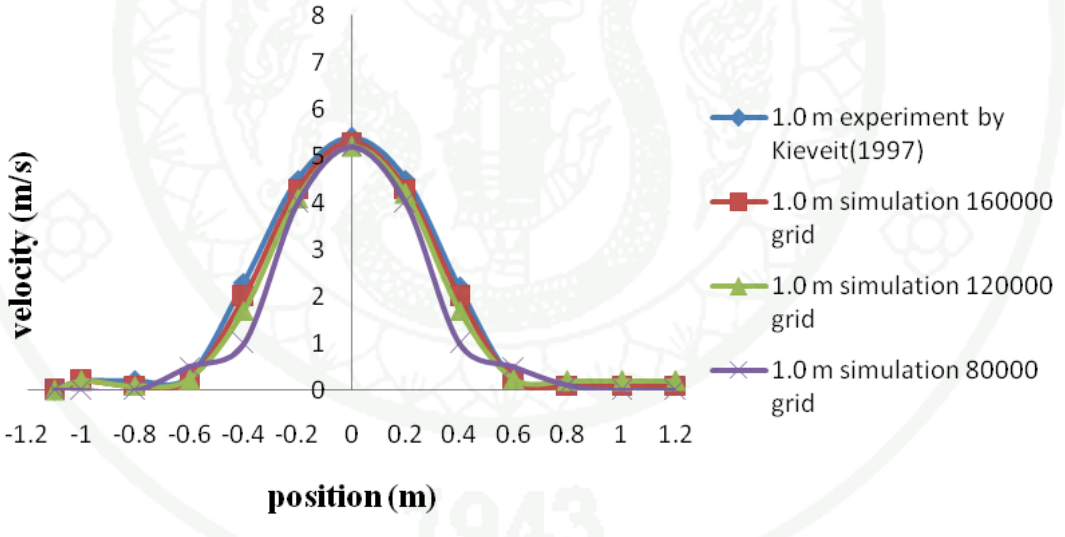

(c)

Appendix Figure D1 (Continued)

Appendix Table D2 Sum error of air temperature profile at different levels of spray chamber

Number of grid / Distance(m)	80,000	120,000	160,000
0.3	13.5 %	4.9 %	4.1 %
0.6	13.6 %	4.7 %	4.1 %
12.4	11.1 %	4.5 %	3.7 %

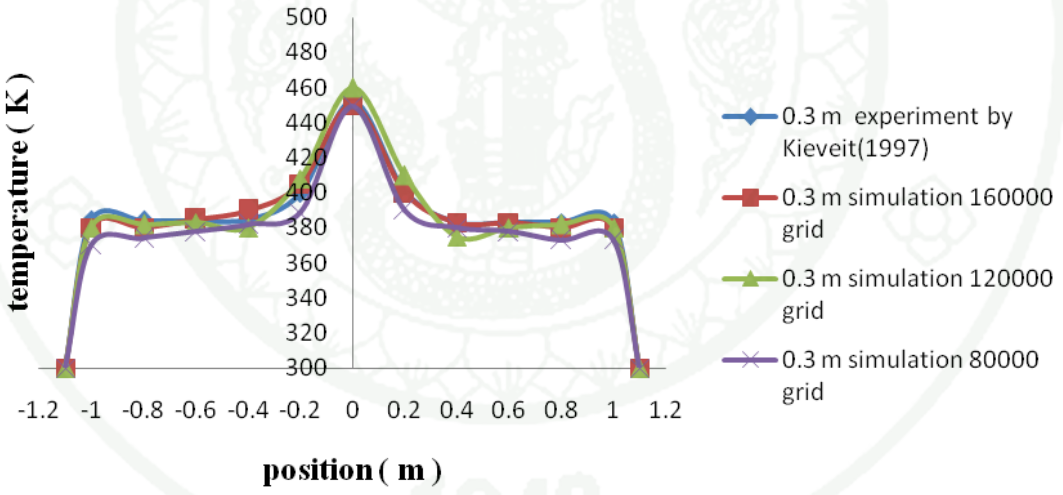

(a)

Appendix Figure D2 Comparison of air velocity profile at different levels of the spray chamber (a) 0.3 m, (b) 0.6 m, (c) 1.0 m. validation between simulation and experiment by Kieveit (1997) very number of grid at 80,000 , 120,000 and 160,000

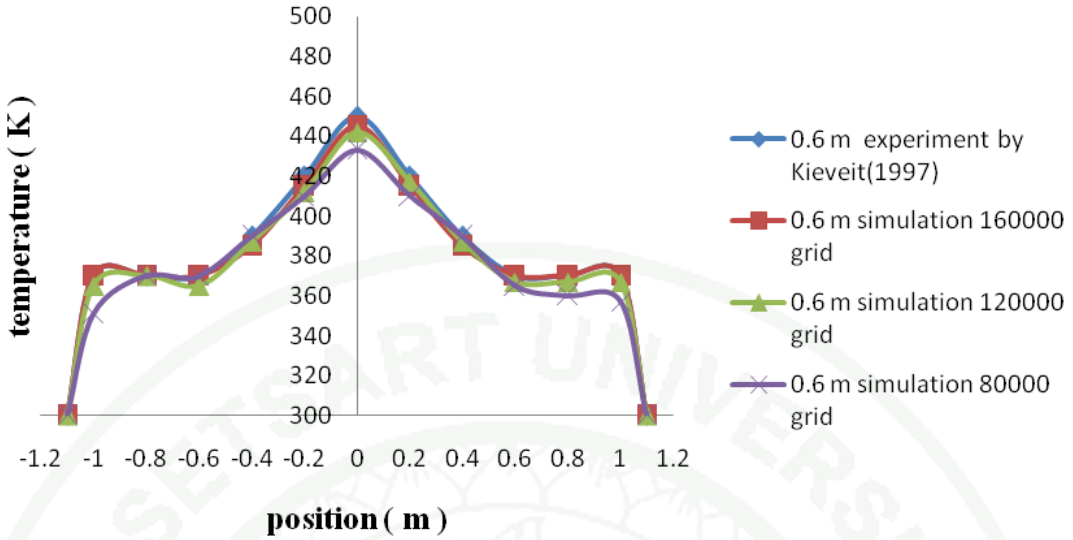

(b)

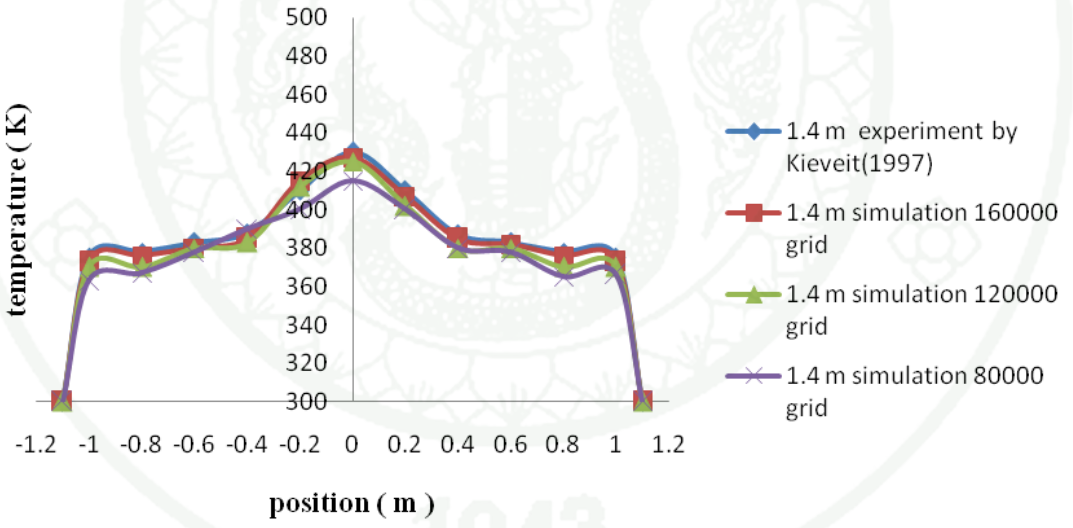

(c)

Appendix Figure D2 (Continued)

CURRICULUM VITAE

NAME : Miss Pornpen Nualnuk

BIRTH DATE : April 9, 1986

BIRTH PLACE : Suratthani, Thailand

EDUCATION :

YEAR	**INSTITUTE**	**DEGREE**
2009	Kasetsart University	B.Eng (Food Eng)